[RhCl(CS)(PPh_3)$_2$], 26500-10-7; [IrCl(CO)(PPh_3)$_2$], 14871-41-1; Fe, 7439-89-6; Rh, 7440-16-6.

Supplementary Material Available: Tables of temperature factors for anisotropic atoms (S-I), hydrogen atom positional parameters (S-II), bond distances (S-III), and bond angles (S-IV) (8 pages); a listing of observed and calculated structure factor amplitudes (×10) for all observed reflections (S-V) (17 pages). Ordering information is given on any current masthead page.

Allene Adducts of Ditungsten Hexaalkoxides. Three Modes of Allene Coordination to Dinuclear Centers As Seen in the Structures of W_2(O-*t*-Bu)$_6$(C_3H_4), W_2(O-*t*-Bu)$_6$(C_3H_4)$_2$, and W_2(O-*t*-Bu)$_6$(C_3H_4)(CO)$_2$

Stephanie T. Chacon, Malcolm H. Chisholm,* Kirsten Folting, John C. Huffman, and Mark J. Hampden-Smith

Department of Chemistry and Molecular Structure Center, Indiana University, Bloomington, Indiana 47405

Received April 5, 1991

Hydrocarbon solutions of W_2(O-*t*-Bu)$_6$ and allene (1 equiv) react at 0 °C to give the monoallene adduct W_2(O-*t*-Bu)$_6$(C_3H_4) (1). Reactions involving W_2(O-*t*-Bu)$_6$ and an excess of allene (>10 equiv) yield the 2:1 adduct W_2(O-*t*-Bu)$_6$(C_3H_4)$_2$ (2). Compound 1 reacts with allene (>10 equiv) and CO (>2 equiv) to yield 2 and W_2(O-*t*-Bu)$_6$(C_3H_4)(CO)$_2$ (3), respectively. A monoallene adduct involving methylallene and W_2(O-*t*-Bu)$_6$ has also been prepared, but reactions involving other W_2(OR)$_6$ compounds where R = *i*-Pr, *c*-Hex, *c*-Pen, and CH_2-*t*-Bu all yield 2:1 adducts, W_2(OR)$_6$(C_3H_4)$_2$. The molecular structures of 1–3 have been determined by low-temperature single-crystal X-ray crystallography. Crystal data for 1: monoclinic, $P2_1/n$, a = 11.676 (1) Å, b = 16.771 (2) Å, c = 17.116 (2) Å, β = 90.39 (0)°, Z = 4. For 2: monoclinic, $P2_1/c$, a = 9.516 (3) Å, b = 19.114 (7) Å, c = 19.438 (6) Å, β = 103.32 (2)°, Z = 4. For 3: monoclinic, $P2_1/c$, a = 15.823 (4) Å, b = 18.807 (5) Å, c = 22.457 (6) Å, β = 90.93 (1)°, Z = 8. The monoallene adduct 1 has a μ-parallel-bridged allene with C–C–C = 141° and W–W = 2.583 (1) Å, W–CH_2 = 2.13 (1) Å, W–C = 2.09 (1) Å, and C–CH_2 = 1.47 (1) Å. This novel $W_2(\mu$-$C_3H_4)$ skeleton is supported by six terminal O-*t*-Bu ligands, three at each W center, W–O = 1.90 (2) Å (average). By contrast, the molecular structure of 2 shows a central $W_2(\mu$-η^1,η^3-$C_3H_4)$ group with an attendant η^2-allene ligand at one metal center. The W–W distance is 2.855 (1) Å and is supported by two bridging alkoxide ligands. The structure of 3 is related to that of 2 by the substitution of the terminal η^2-allene by two η^1-CO ligands. The W–W distance is 3.012 (4) Å, and the two O-*t*-Bu bridges are asymmetric with W–O = 1.99 (3) and 2.30 (4) Å (average), where the long W–O distances are trans to the CO ligands. The bonding in 3 may be viewed as W(6+)---W(2+) where the two CO ligands bond to a pseudooctahedral d^4 metal center. The present work complements earlier studies involving the reactions between W_2(OR)$_6$ compounds with ethylene and alkynes, and the bonding in these adducts has been investigated by qualitative and semiempirical MO approaches.

Introduction

Much of organometallic chemistry owes its existence to an inorganic template. One can think of the spectacular growth during the 1960s and '70s of the organometallic chemistry of the group 8–10 elements that exploited d^6, d^8, and d^{10} ML_n fragments for which tertiary phosphines and phosphites played a ubiquitous ancillary role. More recently, but equally spectacular, has been the organometallic chemistry supported by the d^0, d^2-bent Cp_2M and Cp^*_2M fragments. The work of Bercaw, Marks, and others with the early transition metals, the group 3 elements (Sc, Y), and the lanthanides and actinides has opened up an organometallic chemistry that had lain barren for decades and could not have been developed but for the use of Cp and Cp* ligands. Our efforts are aimed at developing organometallic chemistry of dinuclear systems containing M–M multiple bonds. A particularly attractive group of compounds has the formula M_2(OR)$_6$ where M = Mo and W and R = alkyl or aryl. These are coordinatively unsaturated, and the metal centers are Lewis acidic, yet the presence of the M≡M bond affords an electron reservoir for π-acid ligands and redox chemistry.[1] The selection of M, Mo vs W, and R influences both steric and electronic factors, and thus a M_2(OR)$_6$ compound can be made substrate selective. As part of our continuing investigations of the reactivity of W_2(OR)$_6$ compounds toward unsaturated organic molecules, we have examined reactions involving allene and methylallene. We describe herein our findings. Preliminary reports have appeared.[2,3]

Results and Discussion

Syntheses. W_2(O-*t*-Bu)$_6$ and allene (1 equiv) react in hexane at 0 °C to give W_2(O-*t*-Bu)$_6$(C_3H_4) (1), which crystallizes at −72 °C (dry ice/EtOH), as dark green blocks (cubes). Crystals suitable for an X-ray study were obtained from Et_2O at −72 °C. Compound 1 is thermally unstable in solution above 0 °C, and the decomposition products W_2(O-*t*-Bu)$_6$ and (*t*-BuO)$_3$W≡CMe[4] have been identified by NMR spectroscopy. Even in the crystalline state, compound 1 decomposes slowly (24 h) at room temperature, ca. 25 °C. However, when stored in the solid state at −20 °C it appears indefinitely stable, ca. 1 year. Com-

(1) Chisholm, M. H. *New. J. Chem.* **1987**, *6*, 459.

(2) Cayton, R. H.; Chisholm, M. H.; Hampden-Smith, M. J. *J. Am. Chem. Soc.* **1988**, *110*, 4438.

(3) Cayton, R. H.; Chacon, S. T.; Chisholm, M. H.; Hampden-Smith, M. J.; Huffman, J. C.; Folting, K.; Ellis, P. D.; Huggins, B. A. *Angew. Chem., Int. Ed. Engl.* **1989**, *28*, 11; *Angew. Chem.* **1989**, *101*, 1547.

(4) Listemann, M. L.; Schrock, R. R. *Organometallics* **1985**, *4*, 74.

0276-7333/91/2310-3722$02.50/0

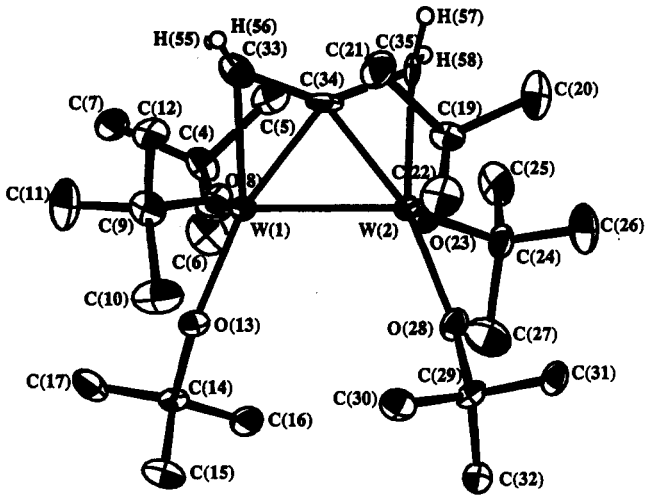

Figure 1. ORTEP diagram of $W_2(O\text{-}t\text{-}Bu)_6(C_3H_4)$ (1), showing the atom number scheme. Thermal ellipsoids are shown at 50%. This view is perpendicular to the W–W axis and shows how the three allene carbon atoms and the two tungsten atoms all lie essentially in the same plane. Protons of the O-*t*-Bu groups have been omitted for clarity.

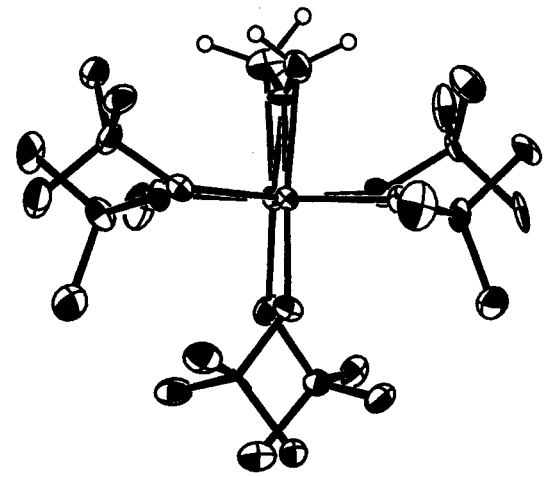

Figure 2. ORTEP diagram of $W_2(O\text{-}t\text{-}Bu)_6(C_3H_4)$ (1) with 50% thermal ellipsoids. This view is down the W–W bond axis. Note the rehybridization of the allene fragment so that the four allene protons now lie essentially in the same plane. The O-*t*-Bu protons have been omitted for clarity.

pound 1 is, like all other compounds described in this work, air and moisture sensitive and must be handled under an inert atmosphere (N_2) with dry and deoxygenated solvents.

$W_2(O\text{-}t\text{-}Bu)_6$ and allene (>10 equiv) react in hexane solutions at 0 °C to give $W_2(O\text{-}t\text{-}Bu)_6(C_3H_4)_2$ (**2**), which is also green but crystallizes from toluene at −72 °C as thin hexagonal plates. Compound **2** is also thermally unstable above 0 °C.

The reactions between $W_2(OR)_6$ compounds where R = *i*-Pr, *c*-Hex, *c*-Pen, and CH_2-*t*-Bu or $W_2(O\text{-}i\text{-}Pr)_6(py)_2$ and allene (>2 equiv) in hydrocarbon solvents from −78 °C to room temperature yield 2:1 adducts of formula $W_2(OR)_6(C_3H_4)_2$. Even when only 1 equiv of allene is added, the 2:1 adducts are formed, leaving unreacted $W_2(OR)_6$ in addition. We have seen no evidence for the formation of a 1:1 adduct unless R = *t*-Bu. These 2:1 adducts are dark brown or green and stable at room temperature both in solution and in the solid state.

A methylallene adduct was prepared by the addition of $MeCH{=}C{=}CH_2$ to $W_2(O\text{-}t\text{-}Bu)_6$ in hexane at 0 °C. This compound of formula $W_2(O\text{-}t\text{-}Bu)_6(MeCHCCH_2)$ was obtained as green crystals from pentane at −78 °C.

Compound 1 reacts with CO (2 equiv) at 0 °C in hexane or toluene to give $W_2(O\text{-}t\text{-}Bu)_6(C_3H_4)(CO)_2$ (**3**), which was isolated as red crystals from hexane at −20 °C. Compound **3** is thermally stable at room temperature.

Solid-State and Molecular Structures. $W_2(O\text{-}t\text{-}Bu)_6(C_3H_4)$ (1). Compound 1 crystallizes in the space group $P2_1/c$ with four molecules in the unit cell. All of the hydrogen atoms were located during the refinement, and all non-hydrogen atoms were refined anisotropically.

An ORTEP diagram of the unique molecule giving the atom number scheme is shown in Figure 1. This view is perpendicular to the W–W axis, and a view along the W–W axis is given in Figure 2. Atomic coordinates are given in Table I, and selected bond distances and angles are given in Table II.

The most striking feature of the molecule is the presence of the bridging parallel aligned allene. The allene hydrogen atoms lie in essentially one plane; i.e. they are twisted by 90° from the ground-state structure of molecular allene that has D_{2d} symmetry. The allene unit has been rehybridized and no longer consists of two mutually perpendicular π-systems. The C–C–C angle is 141 (1)°, and the C–C distances are 1.47 (1) Å (average). The latter is notably longer than that in free allene, 1.309 (1) Å,[5] and is essentially a C_{sp^2}–C_{sp^2} single bond distance. For example, in acrolein the $H_2C{=}C_{sp^2}(H)$–$C_{sp^2}HO$ distance is 1.472 Å.[6]

The W–W distance is 2.583 (1) Å, notably longer than the distances associated with W–W triple bonds that fall in a narrow range from 2.25 to 2.36 Å.[7] The W–O distances, 1.90 (2) Å (average), are rather typical of W–OR distances in $W_2(OR)_6$ and $W_2(OR)_6L_2$ compounds in which a significant degree of shortening is seen due to O_{p_π} to W_{d_π}

Table I. Atomic Coordinates for $W_2(O\text{-}t\text{-}Bu)_6(C_3H_4)$ (1)

atom	10^4x	10^4y	10^4z	$10B_{iso}$, Å^2
W(1)	9186.8 (3)	406.3 (2)	2066.9 (2)	11
W(2)	10885.4 (3)	1366.9 (2)	2298.2 (2)	11
O(3)	9491 (4)	−458 (3)	2728 (3)	18
C(4)	10101 (6)	−1176 (5)	2906 (5)	18
C(5)	11339 (7)	−1145 (5)	2656 (5)	22
C(6)	10038 (8)	−1279 (5)	3789 (5)	27
C(7)	9448 (7)	−1867 (5)	2510 (5)	20
O(8)	8387 (4)	918 (3)	1258 (3)	14
C(9)	7290 (7)	893 (5)	872 (5)	20
C(10)	6577 (8)	1567 (6)	1202 (6)	32
C(11)	6746 (8)	82 (6)	1046 (6)	34
C(12)	7501 (7)	990 (6)	−8 (5)	22
O(13)	7873 (4)	631 (3)	2706 (3)	16
C(14)	7412 (7)	527 (5)	3468 (4)	15
C(15)	6466 (7)	1160 (5)	3549 (5)	22
C(16)	8237 (8)	687 (5)	4073 (5)	21
C(17)	6894 (7)	−287 (5)	3531 (5)	25
O(18)	10734 (4)	2165 (3)	1540 (3)	16
C(19)	10802 (7)	2432 (5)	742 (4)	15
C(20)	12016 (8)	2748 (5)	627 (5)	24
C(21)	10522 (8)	1771 (5)	184 (5)	26
C(22)	9931 (8)	3098 (6)	665 (5)	25
O(23)	11674 (4)	822 (3)	3103 (3)	15
C(24)	12528 (7)	1028 (5)	3690 (4)	18
C(25)	13282 (7)	293 (5)	3788 (5)	26
C(26)	13214 (8)	1738 (6)	3441 (6)	28
C(27)	11880 (8)	1186 (6)	4449 (5)	31
O(28)	10534 (4)	2169 (3)	3069 (3)	17
C(29)	9928 (7)	2903 (4)	3189 (4)	15
C(30)	8784 (7)	2884 (5)	2781 (5)	21
C(31)	10659 (7)	3592 (5)	2927 (5)	17
C(32)	9725 (7)	2949 (5)	4085 (5)	22
C(33)	10067 (1)	−204 (5)	1158 (5)	20
C(34)	10780 (7)	421 (4)	1515 (5)	19
C(35)	11975 (7)	716 (5)	1514 (5)	19

(5) Stoicheff, B. P. *Can. J. Phys.* **1955**, *33*, 811.
(6) Stoicheff, B. P. *Tetrahedron* **1962**, *17*, 135.
(7) Chisholm, M. H. *Polyhedron* **1983**, *2*, 681.

Table II. Selected Bond Distances (Å) and Angles (deg) for $W_2(O\text{-}t\text{-}Bu)_6(C_3H_4)$ (1)

Distances			
W(1)-W(2)	2.5828 (5)	W(2)-O(28)	1.933 (5)
W(1)-O(3)	1.873 (5)	W(2)-C(34)	2.086 (8)
W(1)-O(8)	1.875 (5)	W(2)-C(35)	2.141 (8)
W(1)-O(13)	1.927 (5)	C(33)-C(34)	1.456 (12)
W(1)-C(33)	2.128 (8)	C(34)-C(35)	1.471 (11)
W(1)-C(34)	2.089 (8)	O-C	1.44 (9) av
W(2)-O(18)	1.866 (5)	C(*t*-Bu)-C(*t*-Bu)	1.52 (1) av
W(2)-O(23)	1.886 (5)		
Angles			
W(2)-W(1)-O(3)	104.03 (16)	W(1)-W(2)-O(18)	105.70 (15)
W(2)-W(1)-O(8)	101.73 (15)	W(1)-W(2)-O(23)	100.66 (15)
W(2)-W(1)-O(13)	113.97 (15)	W(1)-W(2)-O(28)	112.04 (15)
W(2)-W(1)-C(33)	92.08 (23)	W(1)-W(2)-C(34)	51.84 (22)
W(2)-W(1)-C(34)	51.74 (21)	W(1)-W(2)-C(35)	92.26 (20)
O(3)-W(1)-O(8)	153.82 (22)	W(1)-O(3)-C(4)	150.8 (5)
O(3)-W(1)-O(13)	87.59 (22)	W(1)-O(8)-C(9)	140.0 (5)
O(3)-W(1)-C(33)	88.9 (3)	W(1)-O(13)-C(14)	143.3 (5)
O(3)-W(1)-C(34)	96.29 (27)	W(1)-C(33)-C(34)	68.4 (5)
O(8)-W(1)-O(13)	86.23 (21)	W(1)-C(34)-W(2)	76.43 (25)
O(8)-W(1)-C(33)	85.6 (3)	W(1)-C(34)-C(33)	71.2 (5)
O(8)-W(1)-C(34)	95.93 (27)	W(1)-C(34)-C(35)	147.1 (6)
O(13)-W(1)-C(33)	153.79 (27)	C(33)-C(34)-C(35)	140.9 (7)
O(13)-W(1)-C(34)	165.70 (26)	W(2)-C(35)-C(34)	67.6 (4)
C(33)-W(1)-C(34)	40.4 (3)		

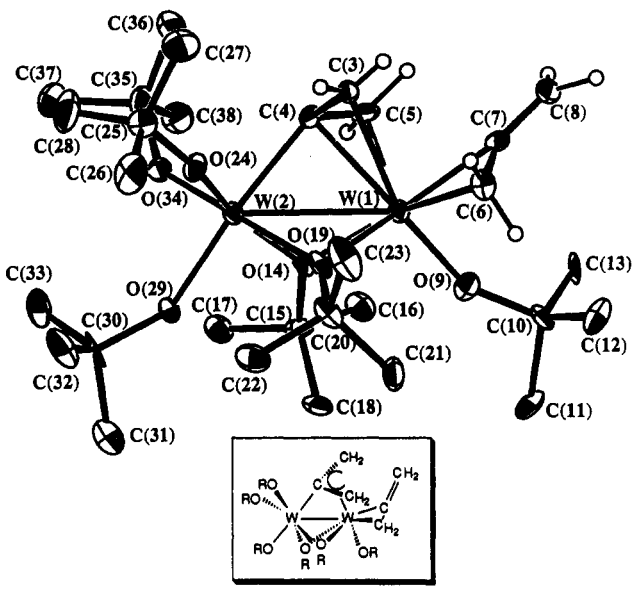

Figure 3. ORTEP diagram and line drawing of $W_2(O\text{-}t\text{-}Bu)_6(C_3H_4)_2$ (2) with 50% thermal ellipsoids and showing the atom number scheme. This view is perpendicular to the W-W bond axis and shows the bridging allene group side-on. The protons of the O-*t*-Bu groups have been omitted for clarity.

bonding. The tungsten–carbon distances 2.13 (1) Å (CH_2) and 2.09 (1) Å (-C-) are quite short relative to W-C_{sp^2} distances (2.14–2.19 Å)[8] and comparable or slightly shorter than the W-C distances, 2.14 (2) Å (average), in the ethylene adduct $W_2(OCH_2\text{-}t\text{-}Bu)_6(\eta^2\text{-}C_2H_4)_2$.[9]

Finally, it is worthy of note that while the allene bridges the two metal atoms, the alkoxide ligands are all terminal such that the W_2O_6 moiety is eclipsed.

$W_2(O\text{-}t\text{-}Bu)_6(C_3H_4)_2$ (2). Compound **2** also crystallized in the space group $P2_1/c$ with four molecules in the unit

Table III. Atomic Coordinates for $W_2(O\text{-}t\text{-}Bu)_6(C_3H_4)_2$ (2)

atom	10^4x	10^4y	10^4z	$10B_{iso}$, Å^2
W(1)	7251.1 (5)	1516.9 (2)	3318.2 (2)	11
W(2)	8676.3 (5)	2701.4 (2)	4061.5 (2)	11
C(3)	7169 (14)	2481 (6)	2542 (6)	18
C(4)	6843 (12)	2652 (6)	3207 (5)	13
C(5)	5509 (12)	2307 (6)	3264 (7)	17
C(6)	7465 (13)	1015 (7)	2328 (6)	20
C(7)	5999 (12)	1166 (6)	2350 (6)	17
C(8)	4692 (13)	1070 (6)	1965 (6)	19
O(9)	6829 (8)	658 (4)	3713 (4)	16
C(10)	6231 (11)	-39 (6)	3666 (5)	15
C(11)	6901 (13)	-393 (6)	4379 (6)	18
C(12)	6657 (14)	-450 (6)	3080 (7)	24
C(13)	4619 (12)	17 (6)	3553 (6)	16
O(14)	7603 (7)	1965 (4)	4447 (3)	13
C(15)	7511 (11)	1685 (6)	5144 (6)	17
C(16)	8679 (12)	1132 (7)	5330 (6)	19
C(17)	7689 (12)	2273 (7)	5694 (6)	18
C(18)	6007 (12)	1376 (6)	5035 (6)	18
O(19)	9398 (7)	1778 (4)	3635 (4)	15
C(20)	10717 (11)	1439 (6)	3544 (6)	16
C(21)	10603 (13)	659 (7)	3699 (7)	23
C(22)	11977 (12)	1744 (7)	4090 (7)	23
C(23)	10911 (12)	1574 (8)	2808 (7)	27
O(24)	9692 (8)	3180 (4)	3505 (4)	16
C(25)	10330 (12)	3771 (6)	3218 (6)	20
C(26)	11903 (15)	3563 (7)	3217 (8)	32
C(27)	9447 (14)	3894 (7)	2475 (7)	29
C(28)	10308 (16)	4396 (7)	3678 (7)	33
O(29)	10211 (8)	2659 (4)	4929 (4)	14
C(30)	11207 (11)	2986 (6)	5503 (5)	17
C(31)	11669 (13)	2452 (7)	6105 (6)	25
C(32)	12524 (13)	3197 (8)	5234 (7)	28
C(33)	10554 (12)	3623 (7)	5761 (7)	23
O(34)	7967 (7)	3489 (4)	4460 (4)	14
C(35)	6773 (13)	3975 (7)	4380 (7)	25
C(36)	6181 (15)	4158 (7)	3600 (7)	32
C(37)	7398 (14)	4650 (7)	4786 (7)	27
C(38)	5597 (12)	3679 (7)	4704 (7)	22

Table IV. Selected Bond Distances (Å) for $W_2(O\text{-}t\text{-}Bu)_6(C_3H_4)_2$ (2)

W(1)-W(2)	2.8548 (10)	W(2)-O(24)	1.849 (7)
W(1)-O(9)	1.894 (7)	W(2)-O(29)	1.961 (7)
W(1)-O(14)	2.306 (7)	W(2)-O(34)	1.887 (7)
W(1)-O(19)	2.055 (7)	W(2)-C(4)	2.117 (11)
W(1)-C(3)	2.372 (11)	C(3)-C(4)	1.434 (16)
W(1)-C(4)	2.206 (11)	C(4)-C(5)	1.458 (16)
W(1)-C(5)	2.227 (12)	C(6)-C(7)	1.436 (17)
W(1)-C(6)	2.201 (12)	C(7)-C(8)	1.308 (16)
W(1)-C(7)	2.092 (11)	O-C	1.45 (1) av
W(2)-O(14)	1.985 (7)	C(*t*-Bu)-C(*t*-Bu)	1.53 (2) av
W(2)-O(19)	2.130 (8)		

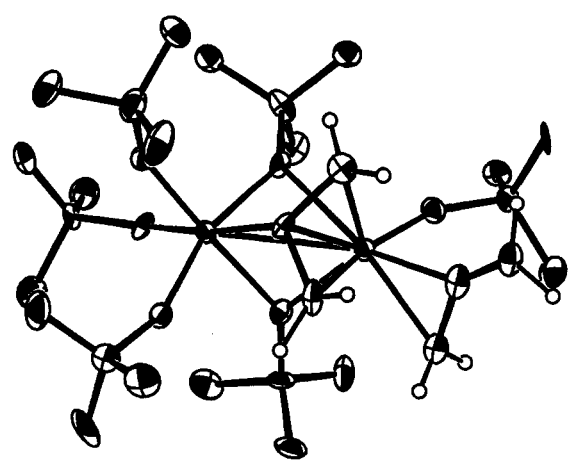

Figure 4. ORTEP diagram of $W_2(O\text{-}t\text{-}Bu)_6(C_3H_4)_2$ (2) with 50% thermal ellipsoids. This view shows the top of the bridging allene group. The protons of the O-*t*-Bu groups have been omitted for clarity.

(8) (a) Chisholm, M. H.; Eichhorn, B. W.; Folting, K.; Huffman, J. C.; Tatz, R. J. *Organometallics* **1986**, *5*, 1599. (b) Chisholm, M. H.; Huffman, J. C.; Hampden-Smith, M. J. *J. Am. Chem. Soc.* **1989**, *111*, 5284.

(9) Cayton, R. H.; Chacon, S. T.; Chisholm, M. H.; Huffman, J. C. *Angew. Chem., Int. Ed. Engl.* **1990**, *29*, 1026; *Angew. Chem.* **1990**, *102*, 1056.

(10) Davis, R. E. *Chem. Commun.* **1968**, 248.

Table V. Selected Bond Angles (deg) for $W_2(O\text{-}t\text{-}Bu)_6(C_3H_4)_2$ (2)

W(2)-W(1)-O(9)	127.08 (22)	W(1)-W(2)-C(4)	50.0 (3)
W(2)-W(1)-O(14)	43.64 (18)	O(14)-W(2)-O(19)	78.4 (3)
W(2)-W(1)-O(19)	48.11 (21)	O(14)-W(2)-O(24)	162.8 (3)
W(2)-W(1)-C(3)	69.39 (28)	O(14)-W(2)-O(29)	89.6 (3)
W(2)-W(1)-C(4)	47.33 (28)	O(14)-W(2)-O(34)	98.5 (3)
W(2)-W(1)-C(5)	75.4 (3)	O(14)-W(2)-C(4)	82.0 (3)
W(2)-W(1)-C(6)	131.3 (3)	O(19)-W(2)-O(24)	85.6 (3)
W(2)-W(1)-C(7)	144.6 (3)	O(19)-W(2)-O(29)	93.29 (28)
O(9)-W(1)-O(14)	86.2 (3)	O(19)-W(2)-O(34)	176.9 (3)
O(9)-W(1)-O(19)	112.2 (3)	O(19)-W(2)-C(4)	86.5 (3)
O(9)-W(1)-C(4)	147.5 (3)	O(24)-W(2)-O(29)	97.9 (3)
O(9)-W(1)-C(6)	92.7 (4)	O(24)-W(2)-O(34)	97.5 (3)
O(9)-W(1)-C(7)	87.5 (4)	O(24)-W(2)-C(4)	90.6 (4)
O(14)-W(1)-O(19)	73.06 (26)	O(29)-W(2)-O(34)	86.9 (3)
O(14)-W(1)-C(4)	73.3 (3)	O(29)-W(2)-C(4)	171.5 (4)
O(14)-W(1)-C(6)	166.1 (4)	O(34)-W(2)-C(4)	92.8 (4)
O(14)-W(1)-C(7)	154.5 (4)	W(1)-O(9)-C(10)	153.1 (7)
O(19)-W(1)-C(4)	86.1 (4)	W(1)-O(14)-C(15)	135.4 (6)
O(19)-W(1)-C(6)	94.7 (4)	W(2)-O(14)-C(15)	138.3 (6)
O(19)-W(1)-C(7)	131.9 (4)	W(1)-O(19)-C(20)	132.8 (6)
C(4)-W(1)-C(6)	113.1 (4)	W(2)-O(19)-C(20)	141.1 (6)
C(4)-W(1)-C(7)	100.1 (4)	W(2)-O(24)-C(25)	158.4 (7)
W(1)-W(2)-O(14)	53.31 (19)	W(2)-O(29)-C(30)	151.7 (7)
W(1)-W(2)-O(19)	45.89 (19)	W(2)-O(34)-C(35)	144.5 (7)
W(1)-W(2)-O(24)	110.35 (23)	W(1)-C(4)-W(2)	82.7 (4)
W(1)-W(2)-O(29)	125.10 (22)	C(3)-C(4)-C(5)	109.8 (10)
W(1)-W(2)-O(34)	131.83 (21)	C(6)-C(7)-C(8)	139.2 (12)

cell. All hydrogen atoms were located in the refinement and were refined isotropically. All non-hydrogen atoms were refined anisotropically. A listing of atomic coordinates is given in Table III. Selected bond distances and bond angles are given in Tables IV and V. An ORTEP diagram of the molecule showing the atomic number scheme is shown in Figure 3. This view is perpendicular to the M–M axis, and a similar view, but at 90° to the first, is shown in Figure 4. The molecule is chiral and in the space group $P2_1/c$ with $Z = 4$; there are two enantiomeric pairs in the unit cell.

The pertinent structural features of this molecule include (1) a bridging allene ligand that may be viewed as a metallaallyl, i.e. μ-η^1,η^3-C_3H_4 (the bridging allene is σ-bonded to W(2) and π-bonded to W(1)), (2) an η^2-allene bonded to W(1), and (3) a pair of bridging alkoxide ligands that span a long W–W bond of distance 2.855 (1) Å. The local coordination about W(2) is pseudooctahedral (ignoring the M–M bond) while that about W(1) may be described as five-coordinate, if the μ-allene and the η^2-allene are each considered to occupy one coordination site. The coordination about W(1) can then be described in terms of a distorted trigonal bipyramid in which the η^2-allene and one of the bridging alkoxides, O(14), occupy formal axial sites. It is noteworthy that the W(1)–O(14) distance, 2.306 (7) Å is much longer than the W(1)–O(19) distance, 2.055 (7) Å, both of which are bridging alkoxide distances. This long W(1)–O(14) distance may result from the high trans influence of the η^2-allene ligand. The C–C distances in the μ-allyl ligand are 1.45 (2) Å (average), and the W(2)–C(4) distance 2.12 (1) Å is notably shorter than the W(1)–η^3-allyl distances that span the range 2.21 (1)–2.37 (1) Å, consistent with the view that W(2)–C(4) involves a tungsten–carbon single bond, C_{sp^2}. The C–C–C angle of the μ-allyl ligand is 110 (1)°. The protons of the μ-allyl ligand again lie within a plane, but this time the plane is that of the μ-C_3 moiety as expected for an allylic system.

The metric parameters for the W(1)–η^2-allene moiety are as expected in mononuclear chemistry. The C–C distance of the noncoordinated double bond is 1.31 (2) Å, close to the value in free allene, while the C–C distance

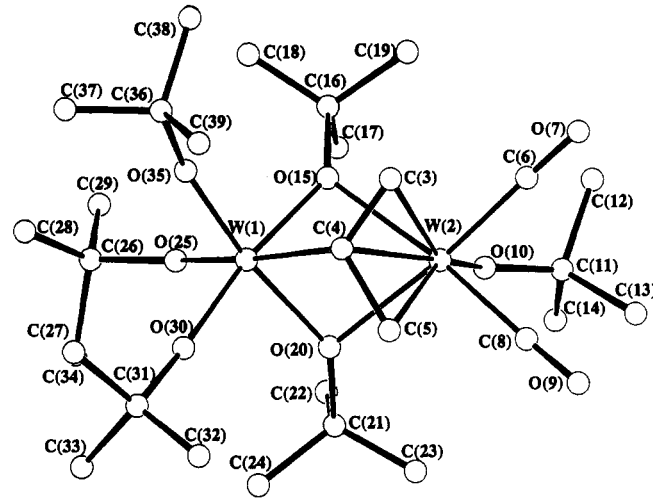

Figure 5. Ball-and-stick drawing of $W_2(O\text{-}t\text{-}Bu)_6(C_3H_4)(CO)_2$ (3), showing the bridging allene group from the top.

of the η^2-carbon atoms is 1.44 (2) Å and the C–C–C angle is 139 (1)°. The W(1)–η^2-distances are 2.20 (1) Å (CH_2) and 2.09 (1) Å (–C–). Despite the bending of the allene on coordination to W(1) the methylene groups remain orthogonal, implying little communication between the two C–C π-systems.

$W_2(O\text{-}t\text{-}Bu)_6(C_3H_4)(CO)_2$ (3). The molecular structure of compound **3** is closely related to that just described for **2**. A ball-and-stick drawing indicating the atom number system is shown in Figure 5. Atomic coordinates are given in Table VI, and listings of pertinent bond distances and angles are given in Tables VII and VIII.

Despite several attempts, the crystals that were examined were less than ideal and the solution of the molecular structure was not as straightforward and successful as would be desired (see Experimental Section for details). Nevertheless the gross features of the structure are unequivocal. That is to say that the W–W distance is 3.012 (4) Å and is supported by two bridging alkoxides and a μ-allyl ligand of the type well characterized for **2**. In addition, the local coordination about W(1) is again pseudooctahedral. At W(2) there is a pair of cis carbonyl ligands, and if the η^3-metallaallyl moiety is considered to occupy one coordination site, then the presence of one terminal OR ligand and the two μ-OR ligands completes a pseudooctahedral geometry. The W–O distances of the μ-OR ligands are notably asymmetric, 1.99 (3) Å to W(1) versus 2.30 (4) Å to W(2). It is thus possible to consider the molecule as the sum of a W(6+) center, W(1), linked to a d^4 *cis*-$(CO)_2W^{2+}$ center. We shall return to this point when we discuss the bonding.

Bonding Discussion and Comparison with Related or Pertinent Structures. Within the structures of **1** and **2** we see three different modes of allene-to-metal bonding, two of which are unique to dinuclear chemistry. The μ-η^1,η^3-bonding mode in **2** and **3** is similar to that first observed by Davis[10] in his structural characterization of the allene–diiron complex $Fe_2(CO)_6(PPh_3)(C_3H_4)$. However, the μ-parallel allene bonding mode seen in **1** is without precedent and worthy of specific attention.

$W_2(O\text{-}t\text{-}Bu)_6(C_3H_4)$. The bonding in **1** lends itself to study by the fragment molecular orbital approach, and it has been examined by the Fenske–Hall MO calculational method. These results were described in a preliminary communication[3] and will not be further discussed here. We prefer to emphasize the essential qualitative features of bonding that can be understood and appreciated without computational aids.

Table VI. Atomic Coordinates for $W_2(O\text{-}t\text{-}Bu)_6(C_3H_4)(CO)_2$ (3)

atom	10^4x	10^4y	10^4z	$10B_{iso}$, Å^2	atom	10^4x	10^4y	10^4z	$10B_{iso}$, Å^2
W(1)	2537 (1)	2194 (1)	7805 (1)	10	W(1)′	2533 (1)	−2709 (1)	4685 (1)	20
W(2)	2501 (1)	3383 (1)	6904 (1)	11	W(2)′	2442 (1)	−1507 (1)	5566 (1)	12
C(3)	3357 (29)	2480 (18)	6574 (27)	0 (8)	C(3)′	1737 (46)	−2468 (28)	5895 (42)	35 (13)
C(4)	2685 (25)	2226 (24)	6846 (20)	8 (7)	C(4)′	2533 (24)	−2653 (21)	5644 (19)	3 (7)
C(5)	1899 (30)	2367 (25)	6494 (24)	14 (9)	C(5)′	3288 (32)	−2407 (24)	5926 (25)	18 (10)
C(6)	3306 (31)	3741 (28)	6338 (25)	23 (9)	C(6)′	1670 (29)	−1258 (26)	6152 (23)	19 (9)
O(7)	3764 (22)	3945 (19)	5992 (17)	27 (7)	O(7)′	1219 (19)	−1110 (17)	6571 (15)	18 (6)
C(8)	1756 (24)	3588 (21)	6213 (19)	8 (7)	C(8)′	3195 (29)	−1142 (26)	6181 (23)	19 (9)
O(9)	1339 (20)	3720 (17)	5809 (15)	22 (6)	O(9)′	3616 (21)	−970 (19)	6585 (17)	28 (7)
O(10)	2358 (19)	4303 (16)	7298 (15)	16 (6)	O(10)′	2369 (18)	−588 (15)	5127 (14)	13 (6)
C(11)	2302 (29)	5013 (25)	7160 (22)	19 (9)	C(11)′	2327 (32)	141 (26)	5288 (24)	24 (9)
C(12)	3156 (32)	5394 (28)	7194 (24)	27 (10)	C(12)′	1910 (42)	511 (36)	4768 (31)	49 (12)
C(13)	1897 (34)	5149 (30)	6531 (25)	30 (10)	C(13)′	1855 (30)	273 (26)	5829 (22)	22 (9)
C(14)	1775 (29)	5404 (26)	7597 (22)	21 (9)	C(14)′	3190 (40)	448 (35)	5332 (30)	46 (12)
O(15)	3286 (15)	3023 (14)	7729 (12)	2 (5)	O(15)′	3281 (18)	−1867 (16)	4797 (14)	12 (6)
O(16)	3943 (28)	3431 (24)	8094 (21)	51 (10)	C(16)′	3974 (27)	−1483 (24)	4502 (20)	15 (8)
C(17)	3498 (34)	3955 (30)	8487 (27)	32 (10)	C(17)′	3584 (31)	−977 (27)	4053 (24)	24 (9)
C(18)	4458 (27)	2927 (25)	8448 (21)	16 (8)	C(18)′	4472 (30)	−1114 (27)	4957 (24)	23 (9)
C(19)	4470 (26)	3809 (23)	7617 (21)	11 (8)	C(19)′	4531 (31)	−2018 (28)	4180 (24)	27 (10)
O(20)	1656 (16)	2928 (15)	7634 (13)	7 (5)	O(20)′	1660 (21)	−1962 (18)	4790 (16)	22 (7)
C(21)	873 (27)	3262 (24)	7900 (20)	15 (8)	C(21)′	917 (24)	−1689 (22)	4510 (19)	8 (7)
C(22)	1148 (36)	3684 (31)	8372 (27)	36 (11)	C(22)′	1241 (25)	−1163 (22)	3988 (20)	10 (7)
C(23)	428 (25)	3646 (23)	7421 (20)	11 (8)	C(23)′	390 (30)	−2241 (28)	4213 (23)	22 (9)
C(24)	320 (31)	2666 (27)	8138 (23)	22 (9)	C(24)′	430 (28)	−1241 (25)	4898 (22)	16 (9)
O(25)	2485 (21)	2300 (20)	8633 (17)	21 (7)	O(25)′	2554 (19)	−2630 (15)	3812 (15)	8 (6)
C(26)	2486 (24)	2031 (21)	9259 (18)	5 (7)	C(26)′	2649 (28)	−2869 (25)	3221 (22)	16 (8)
C(27)	1557 (30)	2077 (27)	9465 (22)	21 (9)	C(27)′	3110 (28)	−2409 (22)	2890 (21)	12 (8)
C(28)	2803 (34)	1296 (30)	9258 (26)	32 (10)	C(28)′	3057 (36)	−3565 (32)	3205 (27)	37 (11)
C(29)	2973 (38)	2529 (27)	9623 (28)	31 (11)	C(29)′	1745 (32)	−2928 (30)	3008 (25)	29 (10)
O(30)	1724 (16)	1482 (15)	7800 (13)	9 (5)	O(30)′	3446 (15)	−3338 (14)	4736 (11)	2 (5)
C(31)	1210 (27)	864 (24)	7711 (21)	15 (8)	C(31)′	4037 (27)	−3850 (24)	4985 (21)	15 (8)
C(32)	743 (37)	965 (33)	7174 (29)	40 (11)	C(32)′	3680 (29)	−4124 (25)	5587 (22)	20 (9)
C(33)	597 (26)	833 (23)	8255 (20)	13 (8)	C(33)′	4900 (34)	−3517 (30)	5110 (25)	33 (10)
C(34)	1761 (39)	207 (35)	7748 (29)	44 (12)	C(34)′	4059 (32)	−4422 (27)	4511 (24)	26 (9)
O(35)	3435 (18)	1550 (16)	7828 (14)	13 (6)	O(35)′	1725 (17)	−3422 (16)	4665 (13)	11 (6)
C(36)	4057 (31)	1047 (27)	7610 (24)	23 (9)	C(36)′	1166 (30)	−4045 (26)	4711 (23)	21 (9)
C(37)	4083 (32)	471 (28)	8066 (24)	27 (10)	C(37)′	1704 (32)	−4664 (28)	4769 (24)	26 (10)
C(38)	4934 (43)	1385 (35)	7615 (31)	48 (12)	C(38)′	652 (35)	−4123 (31)	4141 (27)	35 (11)
C(39)	3784 (35)	800 (30)	6996 (27)	33 (10)	C(39)′	612 (36)	−3880 (33)	5239 (29)	39 (11)

Table VII. Pertinent Bond Distances (Å) for $W_2(O\text{-}t\text{-}Bu)_6(C_3H_4)(CO)_2$ (3)

W(1)–W(2)	3.015 (3)	W(2)–C(4)	2.20 (4)
W(1)–O(15)	1.967 (26)	W(2)–C(5)	2.32 (5)
W(1)–O(20)	1.994 (27)	W(2)–C(6)	1.94 (5)
W(1)–O(25)	1.87 (4)	W(2)–C(8)	1.97 (4)
W(1)–O(30)	1.857 (27)	O(7)–C(6)	1.14 (6)
W(1)–O(35)	1.87 (3)	O(9)–C(8)	1.14 (5)
W(1)–C(4)	2.17 (4)	C(3)–C(4)	1.32 (7)
W(2)–O(10)	1.96 (3)	C(4)–C(5)	1.49 (6)
W(2)–O(15)	2.315 (26)	O–C	1.45 (7) av
W(2)–O(20)	2.298 (27)	C(*t*-Bu)–C(*t*-Bu)	1.50 (8) av
W(2)–C(3)	2.30 (4)		

Table VIII. Pertinent Bond Angles (deg) for $W_2(O\text{-}t\text{-}Bu)_6(C_3H_4)(CO)_2$ (3)

O(15)–W(1)–O(2)	81.7 (11)	O(15)–W(2)–C(5)	106.8 (14)
O(15)–W(1)–O(25)	92.2 (14)	O(15)–W(2)–C(6)	106.1 (17)
O(15)–W(1)–O(30)	171.6 (11)	O(15)–W(2)–C(8)	173.4 (13)
O(15)–W(1)–O(35)	93.2 (12)	O(20)–W(2)–C(3)	107.9 (14)
O(15)–W(1)–C(4)	79.4 (13)	O(20)–W(2)–C(4)	75.7 (13)
O(20)–W(1)–O(25)	94.3 (14)	O(20)–W(2)–C(5)	74.7 (14)
O(20)–W(1)–O(30)	90.9 (11)	O(20)–W(2)–C(6)	174.5 (16)
O(20)–W(1)–O(35)	169.5 (12)	O(20)–W(2)–C(8)	106.7 (13)
O(20)–W(1)–C(4)	82.9 (14)	C(4)–W(2)–C(6)	102.5 (19)
O(25)–W(1)–O(30)	92.4 (14)	C(4)–W(2)–C(8)	103.0 (16)
O(25)–W(1)–O(35)	95.0 (14)	C(6)–W(2)–C(8)	78.8 (19)
O(25)–W(1)–C(4)	171.5 (16)	W(2)–O(10)–C(11)	140 (3)
O(30)–W(1)–O(35)	93.4 (12)	W(1)–O(15)–W(2)	89.1 (10)
O(30)–W(1)–C(4)	95.7 (14)	W(1)–O(15)–C(16)	139.4 (24)
O(35)–W(1)–C(4)	87.2 (14)	W(2)–O(15)–C(16)	129.6 (23)
O(10)–W(2)–O(15)	87.8 (11)	W(1)–O(20)–W(2)	89.0 (10)
O(10)–W(2)–O(20)	86.2 (11)	W(1)–O(20)–C(21)	141.5 (24)
O(10)–W(2)–C(3)	150.5 (14)	W(2)–O(20)–C(21)	127.9 (23)
O(10)–W(2)–C(4)	156.6 (15)	W(1)–O(25)–C(26)	154 (3)
O(10)–W(2)–C(5)	149.0 (15)	W(1)–O(30)–C(31)	168.2 (26)
O(10)–W(2)–C(6)	94.1 (18)	W(1)–O(35)–C(36)	159 (3)
O(10)–W(2)–C(8)	96.3 (15)	W(1)–C(4)–W(2)	87.2 (16)
O(15)–W(2)–O(20)	68.4 (9)	C(3)–C(4)–C(5)	111 (4)
O(15)–W(2)–C(3)	74.4 (16)	W(2)–C(6)–O(7)	178 (5)
O(15)–W(2)–C(4)	71.8 (13)	W(2)–C(8)–O(9)	178 (4)

The $W_2(OR)_6$ molecule, A, is coordinatively unsaturated and capable of picking up donor ligands, as in the formation of Lewis base adducts $W_2(OR)_6L_2$, B. There is no

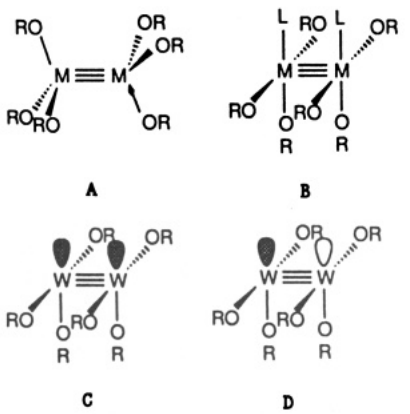

restriction with regard to the conformational preference in Lewis base adducts of type B. Both staggered and eclipsed conformers are known and are equally acceptable for a M–M triple bond, $\sigma^2\pi^4$.[7] Thus we can anticipate the inorganic $M_2(OR)_6$ template of B and its interaction with the allene ligand. The acceptor orbitals are metal centered and are the in- and out-of-plane combinations, as shown in C and D, respectively.

The allene orbitals for a planar V-shaped fragment consist of three carbon 2p orbitals that are contained in one plane and interact to form bonding, nonbonding, and antibonding combinations shown in E, F, and G. In addition there is a noninteracting carbon p orbital that is centered on the tertiary carbon atom, H, and this is orthogonal to the other three.

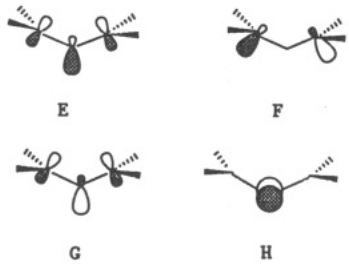

When the two fragments are brought together to form the μ-parallel allene adduct, 1, the allene can act as a four-electron donor: E and F can donate to C and D, respectively. In addition the W–W triple bond can interact with the remaining allene orbitals. Specifically, the W–W π bonds drawn in I and J can mix with G and H.

On the basis of electron occupation, the interactions between I and G and between J and H represent metal to allene π-back-bonding and the interaction between I and G will weaken the C–C bond. On the basis of overlap considerations, the interaction between J and H is the weakest. In the calculation, the in-phase and out-of-phase combinations of J with H constituted the HOMO and LUMO, respectively.

In summary we can see that the μ-parallel allene bonding mode in 1 affords a complete mixing of allene pπ orbitals with those on the W_2 center and readily accounts for the C_{sp^2}—C_{sp^2} single-bond distance.

It is interesting to compare the bonding described above with that for a hypothetical μ-perpendicular allene fragment, as indeed was initially proposed on the basis of NMR data and bonding considerations.[2] In this situation E and H find their match with C and D, respectively. Allene can therefore still act as a four-electron donor to the W_2 center. H can mix with M–M π^*, the out-of-phase combination of I. F can also interact with the in-phase M–M π combination J, but there is no possible interaction with the allene orbital G. Thus, without seeking computational aid, one must conclude that the μ-parallel allene bonding configuration would be favored.

In the $Cp_2Mo_2(CO)_4(C_3H_4)$[11] molecule, allene was seen to straddle the M–M bond in an oblique manner, as shown in K. The bonding here can be described in terms of two orthogonal metal olefin interactions and does not require a rehybridization of the allene in the manner seen in 1. The C–C distances in K are slightly shorter, 1.41–1.44 Å, and the Mo–C(allene) distances notably longer, 2.23 (2) Å (CH_2) and 2.11 (1) and 2.13 (1) Å (–C–). Also, the C–C–C angle is larger, 146 (1)°, in $Cp_2Mo_2(CO)_4(C_3H_4)$, which taken collectively implies a weaker bonding interaction than that in 1.

Another molecule worthy of mention is the 1:1 adduct of di-*p*-tolylcarbodiimide and W_2(O-*t*-Bu)$_6$.[12] This too has

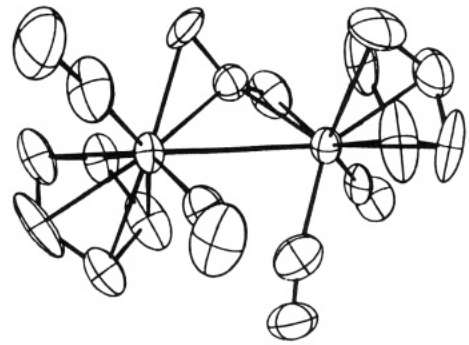

K

a parallel alignment of the N–C–N moiety with the W–W axis and the same disposition of O-*t*-Bu ligands as seen for 1. However, the carbodiimide contains four more electrons and the bonding description is by no means the same as that in 1 because the substituents at nitrogen lie (roughly) in the plane of the N–C–N unit. Thus the carbodiimide N–W bond distances, 2.12 (1) Å, and the W–C distance, 2.21 (2) Å, are notably longer than those in 1 and the N–C–N angle of 154.0 (2)° is only 26° from linearity. The W–W distance of 2.482 (1) Å is also notably shorter than 2.583 (1) Å in 1.

W_2(O-*t*-Bu)$_6$(C_3H_4)$_2$. Let us for the sake of counting electrons assign W(2) the oxidation state +6. It is coordinated to five OR ligands, and even though two are bridging, we will count them as belonging to W(2). Also the W(2)–C(4) bond distance of 2.12 (1) Å is as expected for a W–C_{sp^2} distance and W(2) may be viewed as taking the place of the hydrogen atom of a π-allyl moiety. This then leaves W(1) coordinated to one terminal OR ligand and a π-allyl group, both of which we shall call –1 (uninegative) ligands. The oxidation state of W(1) is thus W(2+), and as noted before, the geometry (ignoring any M–M bonding) is a distorted trigonal bipyramid with the η^2-allene ligand and the long W(1)–O(14) bonded alkoxide ligand in the mutually trans axial positions. Up to this point we have counted the η^2-allene as neutral and considered it to occupy a single coordination site. In a trigonal-bipyramidal field the d orbital splitting is (d_{z^2}) ($d_{x^2-y^2}$, d_{xy}) and (d_{xz}, d_{yz}) with the latter lying lowest in energy since they have no M–L σ character. With W(1) being a d^4 center the d_{xz}, d_{yz} orbitals will be occupied. One of the d_{xz} or d_{yz} will be involved in back-bonding to the η^2-allene ligand. In a true trigonal field the allene would be free to rotate since the d_{xz} and d_{yz} are degenerate. However, in 2 the degeneracy is removed by the low symmetry but more importantly by the fact that only one of the d_{xz} or d_{yz} may be used in M–M bonding. With the assignment of oxidation states W(6+) and W(2+), we therefore would formulate a W(1) to W(2) dative bond (2.855 (1) Å) involving a t_{2g} type orbital on W(2) (acceptor) and one of the d_{xz}, d_{yz} orbitals on W(1) (donor). The whole point of this discussion is to emphasize that $W_{d\pi}$–allene π^* back-bonding requires a specific alignment of the η^2-C–C carbon atom, as is observed. Moreover, as we show later, rotation about the allene–metal bond is not observed on the NMR time scale because of the mutual competition of M–M and M–allene bonding. The C–C distance of the η^2-C(7)–C(6) moiety is 1.44 (2) Å, clearly indicating extensive back-bonding from the metal.

W_2(O-*t*-Bu)$_6$(C_3H_4)(CO)$_2$ (3). Again, for the sake of partitioning of charge we shall assign W(1) to be W(6+) and W(2), with only one terminal OR group and the π-allyl ligand, to be W(2+). (We call the μ-allene ligand a π-allyl

(11) Chisholm, M. H.; Rankell, L. A.; Bailey, W. I., Jr.; Cotton, F. A.; Murillo, C. A. *J. Am. Chem. Soc.* **1977**, *99*, 1261; **1978**, *100*, 802.

(12) Cotton, F. A.; Schwotzer, W.; Shamshoum, E. S. *Organometallics* **1985**, *4*, 461.

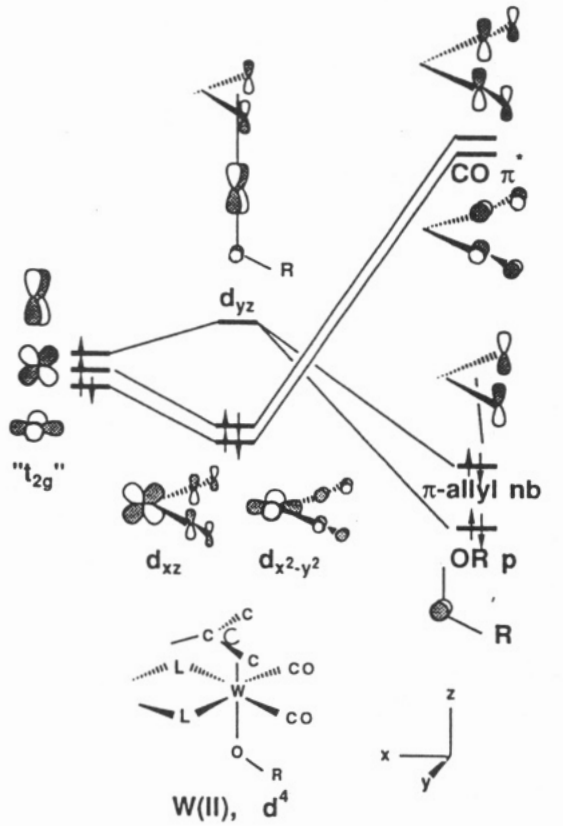

Figure 6. Qualitative molecular orbital diagram for the bonding around W(2) of $W_2(O\text{-}t\text{-}Bu)_6(C_3H_4)(CO)_2$ (**3**).

ligand to W(2) because W(2) is ignorant of the W(1)–C(4) σ-bond.) The coordination about W(1) and W(2) is pseudooctahedral, and W(2) is a d^4 *cis*-$W(CO)_2$-containing complex. As we have seen before,[13] this pseudooctahedral d^4 *cis*-$M(CO)_2$ grouping leads to small C–M–C angles (79° in **3**) for the carbonyl ligands and low values for ν(CO), 1900 and 1830 cm^{-1} in **3**. These can be compared for example with $Mo(O\text{-}t\text{-}Bu)_2(py)_2(CO)_2$,[13] which has trans OR groups and cis CO ligands with C–M–C = 72° and ν(CO) = 1908 and 1768 cm^{-1}. A qualitative MO energy level diagram is shown in Figure 6 for a pseudooctahedral d^4 (π-allyl)$L_2W(OR)(CO)_2$ complex.[14] The key feature of this MO diagram is that for an acute OC–W–CO angle, two of the d_π orbitals are stabilized by the cis CO ligands while the third is destabilized by the allyl nonbonding π orbital and the filled RO p_π orbital. This leads to a significant HOMO–LUMO gap and spin pairing for the d^4 complex. (This is, of course, not common for octahedral d^4 complexes.) Moreover the four metal-based d_π electrons are extensively used in back-bonding to the CO ligands. Thus, in contrast to **2**, there is no reason to formulate a M–M bond in **3**. Note the distance 3.012 (4) Å is longer than that in **2**, 2.855 (1) Å, and the asymmetry of the alkoxides, W(1)–O(15)/O(20) = 1.99 (3) Å versus W(2)–O(15)/O(20) = 2.30 (4) Å. The latter implies RO dative bonds to W(2), consistent with our formulation of the d^4 W(allyl)-(OR)$L_2(CO)_2$ species, where L = a neutral donor ligand.

NMR Studies. The ^1H NMR spectrum of **1** in CD_2Cl_2 at −20 °C shows the expected 2:1 signals for the *t*-BuO ligand and a single resonance for four equivalent protons

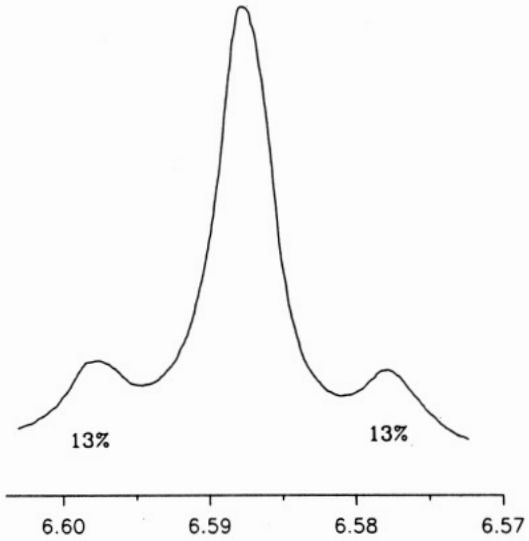

Figure 7. Part of the ^1H NMR spectrum of $W_2(O\text{-}t\text{-}Bu)_6(C_3H_4)$ (**1**), in CD_2Cl_2 at −20 °C, showing the allene proton flanked by 26% intensity satellites from coupling to ^{183}W, $I = {}^1/_2$, 14.5% natural abundance. The scale shows chemical shifts in ppm.

for the allene protons at δ 6.59. The latter signal is temperature independent and is flanked by satellites due to coupling to ^{183}W, $I = {}^1/_2$, 14.5% natural abundance; $^2J_{^{183}W-^1H} = 6.2$ Hz. The relative intensity of the satellietes (26%) appears too large for this to be due to a W–CH_2 interaction; rather it is more in line with each CH_2 group seeing the two W centers equivalently. See Figure 7. In the ^{13}C NMR spectrum there are also signals assignable to the two types of *t*-BuO ligands and the μ-*C* and –CH_2 signals appear at δ 249.7, $J_{^{183}W-^{13}C} = 31$ Hz, and δ 89.1, $J_{^{183}W-^{13}C} = 33$ Hz, $J_{^{13}C-H} = 156$ Hz, respectively. Again, the appearance of the tungsten satellite signals was roughly of 24% intensity in both instances. The bridging tertiary carbon atom should show such relative integral satellites since it has a statistically greater chance of being bound to one ^{183}W nucleus. However, the appearance of the satellite spectra for the CH_2 groups, both ^1H and ^{13}C, are a mystery. Originally, we suggested a μ-perpendicular mode of bonding for a rehybridized allene. The crystal structure clearly shows this to be incorrect, and moreover, the solid-state ^2H NMR spectra of the CD_2CCD_2 isotopically substituted **1** showed that, in the solid-state, the allene-d_4 ligand was rigid on the ^2H NMR time scale.[3] We cannot, however, discount the fact that in solution the allene in **1** is fluxional to the extent that each CH_2 unit sees the two tungsten atoms equivalently. This could be brought about by a rapid μ-parallel $\rightleftarrows$ μ-perpendicular exchange, and as we have shown earlier, this is a symmetry-allowed process although the μ-perpendicular bridge species is anticipated to be a higher energy intermediate or transition state.[3]

In an attempt to interrogate the system further in regard to this process, we tried to prepare a 1:1 allene adduct of $W_2(OR)_5(OR')$ or $W_2(OR)_4$(binaphthalate*).[15] These experiments were unsuccessful in giving the desired compound. Finally, we prepared a 1:1 adduct involving MeCH=C=CH_2. This compound, like **1**, was thermally unstable above 0 °C in solution. However, in the temperature range 0 to −78 °C in toluene-d_8 this 1:1 adduct showed six O-*t*-Bu signals in the ratio 1:1:1:1:1:1. This is consistent with an anticipated μ-parallel structure (based

(13) Chisholm, M. H.; Huffman, J. C.; Kelly, R. L. *J. Am. Chem. Soc.* **1979**, *101*, 7615.

(14) The coupling of cis-CO ligands is described: Hoffmann, R.; Wilker, C. N.; Lippard, S. J.; Templeton, J. L.; Brower, D. C. *J. Am. Chem. Soc.* **1983**, *105*, 146.

(15) Heppert, J. A.; Dietz, S. D.; Boyle, T. J.; Takusagawa, F. *J. Am. Chem. Soc.* **1989**, *111*, 1503.

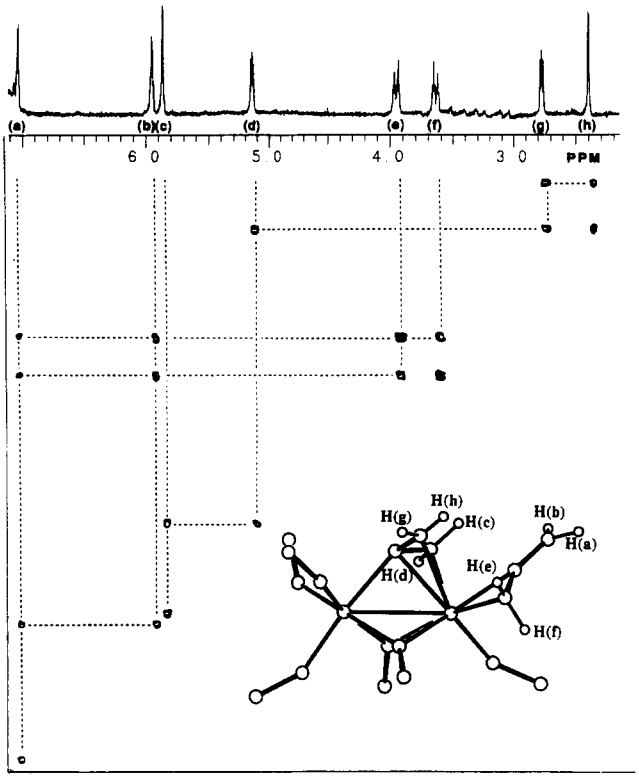

Figure 8. COSY NMR spectrum of $W_2(O\text{-}t\text{-}Bu)_6(C_3H_4)_2$ (2), showing proton correlations as off-diagonal peaks. A ball-and-stick diagram for the $W_2(OC)_6(C_3H_4)_2$ skeleton of 2 showing the assignment of the allenic protons is also given.

on 1) in which the μ-MeCHCCH$_2$ ligand is rigid on the NMR time scale. Thus while we cannot rule out a rapid μ-parallel $\rightleftarrows$ μ-perpendicular exchange for 1, we are inclined to the view that the satellite intensity for the CH_2 groups arises from accidental degeneracy or near equivalence of coupling to the tungsten nuclei, i.e. $^2J_{^{183}W\text{-}^1H} \approx {}^3J_{^{183}W\text{-}^1H}$ and $^1J_{^{183}W\text{-}C} \approx {}^2J_{^{183}W\text{-}^{13}C}$.

$W_2(OR)_6(C_3H_4)_2$ Compounds. The ^{1}H NMR spectra for compound 2 and related bis allene adducts where R = *i*-Pr, *c*-Hex, *c*-Pen, and CH_2-*t*-Bu are qualitatively very similar. In each instance there are six different OR groups and there are eight multiplets for the allene protons. COSY experiments revealed that the eight multiplets of the allene protons were actually composed of two independent sets of ABCD spin systems (see Figure 8). The ^{1}H signals associated with the allene ligands in compound 2 are shown in Figure 8. We have also obtained the ^{13}C NMR spectra for these compounds with and without proton coupling and by the use of the 2D experiment XHCOR. The latter correlates ^{1}H and ^{13}C chemical shifts via ^{13}C–^{1}H couplings. In addition we have carried out NOE difference spectroscopy and spin-saturation transfer experiments. With the combined NMR studies we are able to determine that the η^2-allene is rigid on the NMR time scale; i.e. the allene does not hop from one C–C double bond to the other as is often seen for η^2-allene complexes,[16] and we can make an assignment for all the allene protons. The assignment of protons a, b, c, d, e, f, g, and h is as shown in Figure 8. The protons (a, b), (c, d), (e, f), and (g, h) are all geminal pairs. A NOE was observed (3–5%) between the interior, the anti protons of the μ-η^1,η^3-allene ligand, c and h, and between b and c. The latter involves the two different allene ligands. From the X-ray structure these H---H distances are slightly less than 2.5 Å. A NOE was not observed between any other allene protons (except for geminal pairs), and in all instances the H---H distances are expected to be greater than 2.6 Å.

In the reactions leading to the 2:1 allene adducts where R = *c*-Hex, *i*-Pr, and CH_2-*t*-Bu, there is a kinetic isomer that is formed first, and this only slowly (1–2 h, 0 °C) isomerizes to the thermodynamic isomer. The ^{1}H NMR spectra for the allene region of the thermodynamic products, where R = *t*-Bu, *i*-Pr, *c*-Hex, *c*-Pen, and CH_2-*t*-Bu, were all essentially the same although the relative chemical shifts vary somewhat, and direct comparisons of similar resonances have been made. The NMR data for the kinetic products are qualitatively the same as for the thermodynamic isomer except that the geminal coupling was unobserved for one of the bridging allene geminal pairs. In comparison with Figure 8, the kinetic isomer shows an interallene NOE between e and h (rather than b and c).

We propose that the relationship between the kinetic and thermodynamic products is as shown in L and M, respectively.

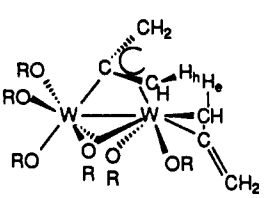

L

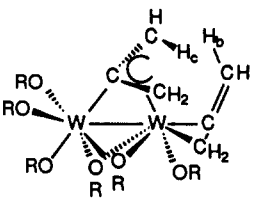

M

The isomerization that takes L to M could be brought about by an allene hop[16] from one double bond to the other or by a pseudorotation of the terminal η^2-allene and W–OR ligands at the pseudo-trigonal-bipyramidal tungsten center. The latter exchanges the asymmetry in the bridging OR ligands as the η^2-allene becomes trans to the μ-OR ligand that was formerly in an equatorial position. While we cannot distinguish between these processes, we can say that allene hopping and/or the pseudorotation must have a fairly high energy of activation ca. $\geq$ 20 kcal mol^{-1}. This is a reflection of the specific binding (M–M vs M–η^2-C_3H_4) requirements, as outlined in an earlier section.

It is interesting that only for $W_2(O\text{-}t\text{-}Bu)_6$ has it proved possible to prepare a 1:1 allene adduct. It seemed likely that this was an intermediate in the synthesis of the 2:1 adduct, 2, and we have found that 2 may be formed from the addition of excess allene to hydrocarbon solutions of 1 at 0 °C. Moreover, we have found that the isotopomer of 1 incorporating allene-d_4 gave upon reaction with protio allene a sample whose ^{1}H NMR spectrum resembled that of 2. Specifically, there were eight allene proton resonances and the spin system was as in Figure 8. However, the integral intensity was only half that of a protio sample of 2. From this we might conclude that there is a reaction that leads to the exchange of the μ-η^1,η^3-allene and the η^2-allene in 2 and that this exchange is slow on the NMR time scale.

We have found no evidence for allene dissociation from 2, and the facts that the conversion of 1 to 2 in the presence of excess allene is sluggish and that analogues of 1 are not seen for alkoxides other than R = *t*-Bu lead us to suspect that the formation of 2 may occur via a symmetrical 2:1 allene adduct of formula $W_2(OR)_6(\eta^2\text{-}C_3H_4)_2$. The structure of this reactive bis(η^2-allene) intermediate might, for example, be similar to $W_2(OCH_2\text{-}t\text{-}Bu)_6(\eta^2\text{-}C_2H_4)_2$[9] or $W_2(OCH_2\text{-}t\text{-}Bu)_6(\eta^2\text{-}OCHCHCHMe)_2$,[17] shown schematically

(16) (a) Ben-Shoshan, R.; Pettit, R. *J. Am. Chem. Soc.* **1967**, *89*, 2231. (b) Vrieze, K.; Volger, H. C.; Gronert, M.; Praat, A. P. *J. Organomet. Chem.* **1969**, *16*, P19. (c) Vrieze, K.; Volger, H. C.; Praat, A. P. *J. Organomet. Chem.* **1970**, *21*, 467.

in N and O. Thus compound 1 may be formed reversibly

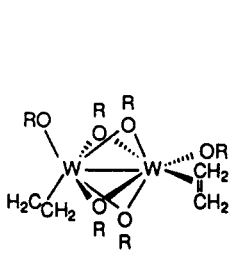

N

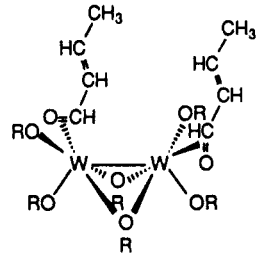

O

from a reactive 1:1 adduct wherein the allene is η^2-bound and it is this 1:1 adduct and not 1 that leads to 2. This process would also account for the appearance of 50:50 allene-d_4 in the μ- and η^2-position of 2 in its synthesis from 1-d_4 and protio allene. Regrettably, we cannot confirm our suspicions.

W_2(O-*t*-Bu)$_6$(μ-C_3H_4)(CO)$_2$ (3). This compound has a virtual mirror plant of symmetry and shows O-*t*-Bu ligands in the ratio 2:2:1:1. The allene protons appear as two singlets, δ 3.60 and 4.05. Apparently, the geminal HH coupling is too small to be observed. There is only one type of CO ligand. In the ^{13}C NMR spectrum of the compound prepared from ^{13}CO the signal at δ 212 with $J_{^{183}W-^{13}C}$ = 180 Hz is readily assignable to the CO group. Rather interestingly, in the ^1H NMR spectrum of this ^{13}CO isotopically substituted sample, only one of the μ-allene signals showed a coupling, $^3J_{^{13}C-^1H}$ = 5 Hz.

The angle between cis CO ligands can be calculated from the ratio of the intensities of the symmetric and antisymmetric bands by using[18]

$$R_{sym}/R_{asym} = \left(\frac{2r\cos\theta}{2r\sin\theta}\right) = \text{cotan}^2\,\theta$$

The calculated value for 3 was 76°. This compares well with the crystallographically obtained value: 79 (2)°.

Other Reactions. Compound 2 and the other related bis(allene) complexes are coordinatively unsaturated and a Lewis base adduct involving $HNMe_2$, W_2(O-*c*-Pen)$_6$(C_3H_4)$_2$($HNMe_2$), has been characterized. The available data indicate that the amine coordinates to the tungsten center that carries the η^2-allene ligand. By NMR spectroscopy, the amine adduct loses $HNMe_2$ reversibly in solution. These compounds also react with CO to give CO adducts which we formulate as $W_2(OR)_6(C_3H_4)_2(CO)$ and $W_2(OR)_6(C_3H_4)(CO)_2$, but these mixtures have not been well characterized.

Concluding Remarks. The allene adducts 1–3 reveal three types of allene-to-metal bonding, two of which are unique to dinuclear chemistry and one of which has not been seen before, namely the μ-parallel mode in 1. This work further exemplifies the versatility of the $W_2(OR)_6$ complexes as templates for organometallic chemistry.

Experimental Section

General Procedures. All preparations were carried out under an inert atmosphere, generally of nitrogen, but also of allene where appropriate, by using standard Schlenk techniques in conjunction with a Vacuum Atmosphere's Co. Dri-Lab system. Aromatic and aliphatic hydrocarbon solvents, diethyl ether, 1,2-dimethoxyethane, and THF, were dried and distilled from sodium benzophenone ketyl and stored over 4-Å molecular sieves. NMR solvents, benzene-d_6, toluene-d_8, and pyridine-d_5, were dried over molecular sieves and degassed with dry nitrogen. Dimethyl-d_6 ether was prepared by the method reported in the literature and then dried and distilled from molecular sieves in vacuo. Freon-12 was purchased from Matheson Chemical Co. and degassed twice before use. A convenient low-temperature NMR solvent system was obtained by mixing Freon-12 and toluene-d_8 in a ratio of approximately 70:30. Alcohols were purchased from Aldrich Chemical Co. 2-Propanol and cyclohexanol were dried and distilled from magnesium turnings and stored over 4-Å molecular sieves. Cyclopentanol and toluene solutions of neopentanol were degassed with dry nitrogen and dried over 4-Å molecular sieves. Allene was purchased from Air Products and used without further purification. 2-Methyl-2-propanol-d_{10} and cyclohexanol-d_{12} were purchased from Aldrich Chemical Co. and were dried over 4-Å molecular sieves for at least 2 days prior to use. Allene-d_4 was purchased from Cambridge Isotopes. W_2(O-*t*-Bu)$_6$[19] and W_2(NMe$_2$)$_6$[20] were prepared by literature procedures and base-free $W_2(OR)_6$, R = cyclohexyl (*c*-Hex), cyclopentyl (*c*-Pen), neopentyl (CH_2-*t*-Bu), and isopropyl (*i*-Pr), were prepared by our recently developed procedure[21] or were generated in situ and used directly. Elemental analyses were carried out by Oneida Research Services, Inc. All samples were handled under an inert atmosphere.

Spectroscopic Instrumentation and Interpretation. ^1H and ^{13}C NMR spectra were recorded on Varian XL300, Nicolet NC360, and Bruker AM500 NMR spectrometers. In some cases ^1H and ^{13}C NMR assignments were made with the aid of a variety of two-dimensional NMR experiments on all three instruments. Typical acquisition parameters were as follows: COSY [512W (8 or 16 scans) × 128]; XHCORR, [1K (84 scans) × 256]. Infrared spectra were recorded on a Perkin Elmer 283 spectrophotometer as Nujol mulls or as KBr discs.

W_2(O-*t*-Bu)$_6$(C_3H_4). W_2(O-*t*-Bu)$_6$ (0.800 g, 1.0 mmol) was placed in a 30-mL Schlenk flask, and 2 mL of hexane was added. The solution was stirred for 15 min at room temperature to break up and dissolve the large crystals of W_2(O-*t*-Bu)$_6$. The suspension was then frozen at −196 °C and the flask evacuated and transferred to a calibrated vacuum manifold. The solution was warmed to 0 °C (still under vacuum) and an excess of allene was added by admitting the gas into the flask via the calibrated manifold. Note: allene is very soluble in hexane even at 0 °C. The solution immediately darkened on addition of allene and had turned dark green after stirring for about 10 min. The solution was stirred for a total of 2 h at 0 °C, during which the red W_2(O-*t*-Bu)$_6$ slowly dissolved to give a deep green solution and a small amount of green precipitate toward the end of this time. The flask was then isolated from the vacuum manifold and placed in a dry ice/acetone bath at −78 °C for 14 h. The contents of the flask were filtered at −78 °C by transferring the supernatant into a new flask cooled to 0 °C. A 632-mg (0.747 mmol) amount of large green crystals was isolated in this way. The filtrate was placed in the dry ice/acetone bath for 24 h, but no more solid material formed. The green crystals isolated were analyzed by a variety of methods and are consistent with the formulation W_2(O-*t*-Bu)$_6$(C_3H_4), obtained in 75% yield. This procedure was repeated several times, and this yield is typical. Care should be taken that the temperature of solution of W_2(O-*t*-Bu)$_6$(C_3H_4) does not exceed 0 °C either in the reaction mixture or solutions of isolated material as other products will be formed. Crystals suitable for a single-crystal X-ray diffraction were obtained from diethyl ether at −72 °C.

^1H NMR data (300 MHz, 0 °C; toluene-d_8, δ): C_3H_4 7.03 (s, J_{H-W} = 6.2 Hz (29%), 4 H); OC(CH_3)$_3$ 1.75 (s, 18 H), 1.28 (s, 36 H); no change in spectrum from 0 to −90 °C in toluene-d_8. ^1H NMR (300 MHz, −60 °C; 70:30 Freon-12:toluene-d_8, δ): C_3H_4 6.72 (s, 4 H); OC(CH_3)$_3$ 1.63 (s, 18 H), 1.20 (s, 36 H). ^1H NMR (300 MHz, −120 °C; 70:30 Freon-12:toluene-d_8, δ): C_3H_4 6.78 (br s); OC(CH_3)$_3$ 1.68 (br s), 1.22 (br s) (protio impurity of methyl resonance of toluene-d_8 also broadened at this temperature).

(17) Chisholm, M. H.; Lucas, E. A.; Sousa, A. C.; Huffman, J. C.; Folting, K.; Labkovsky, E. G.; Streib, W. E. *J. Chem. Soc., Chem. Commun.* **1991**, 847.

(18) Cotton, F. A.; Wilkinson, G. *Advanced Inorganic Chemistry*, 4th ed.; John Wiley & Sons: New York, 1980; pp 1074–1075.

(19) Akiyama, M.; Chisholm, M. H.; Cotton, F. A.; Extine, M. W.; Haitko, D. A.; Little, D.; Fanwick, P. E. *Inorg. Chem.* **1979**, *18*, 2266.

(20) Chisholm, M. H.; Cotton, F. A.; Extine, M.; Stults, B. R. *J. Am. Chem. Soc.* **1976**, *98*, 4477.

(21) Chisholm, M. H.; Hampden-Smith, M. J.; Martin, J. D. *Inorg. Synth.*, submitted for publication.

^{13}C NMR data (75.4 MHz, 0 °C; toluene-d_8, δ): $CH_2{=}C{=}CH_2$ 249.7 (s, $J_{C\text{-}W}$ = 31 Hz (24%); $CH_2{=}C{=}CH_2$ 89.1 (t, $J_{C\text{-}H}$ = 156 Hz, $J_{C\text{-}W}$ = 33 Hz (22%)); $OC(CH_3)_3$ 82.5, 78.0; $OC(CH_3)_3$ 33.5, 31.5.

IR data (cm^{-1}, Nujol mull): 1372 (m), 1369 (s), 1270 (w), 1240 (m), 1181 (s, br), 1032 (m), 1000 (s), 980 (s), 958 (s), 912 (m), 902 (m), 792 (m), 580 (w), 560 (w), 485 (w), 377 (w).

Anal. Calcd for $C_{27}H_{58}O_6W_2$: C, 38.30; H, 6.90. Found: C, 38.24; H, 6.74.

$W_2(OC(CD_3)_3)_6(C_3H_4)$. This compound was prepared in a manner analogous to that described above for the fully protio analogue, by the reaction of $W_2(OC(CD_3)_3)_6$ with allene at 0 °C. The green crystals isolated were characterized by spectroscopic techniques and by combustion analysis. These experiments confirmed that the only ^1H NMR resonance exhibited by allene-derived protons occurs at 7.03 ppm. There are no allene-derived proton signals obscured by the $OC(CH_3)_3$ resonances.

Anal. Calcd for $C_{27}H_4D_{54}O_6W_2$: C, 35.77; H + D (as H), 6.69. Found: C, 36.02; H + D (as H), 6.49.

Rearrangement of $W_2(OC(CD_3)_3)_6(C_3H_4)$. The rearrangement of pure $W_2(O\text{-}t\text{-}Bu)_6$(allene) above 0 °C was most easily monitored by using the compound in which all the tertiary butoxide ligands were deuterium labeled. This results in greater sensitivity by ^1H NMR spectroscopy in tracing the fate of the allene protons.

$W_2(OC(CD_3)_3)_6(C_3H_4)$ in Toluene-d_8. On standing for 18 h at 23 °C, $W_2(OC(CD_3)_3)_6(C_3H_4)$ rearranged fairly clearly to give two major species. The major ^1H NMR resonance was a singlet at δ 3.91, $J_{H\text{-}W}$ = 7.8 Hz (30%), together with a much smaller singlet resonance at δ 16.93, $J_{H\text{-}W}$ = 12 Hz (35%). The ratio of these two resonances was measured as 22.1:0.9, respectively. In the $^{13}C\{^1H\}$ NMR spectrum, allene-derived resonances were observed at δ 254 and 48. Reactions employing the fully protio derivative show the presence of two types of O-*t*-Bu ligands at δ 1.60 and 1.42 in a 2:1 ratio, respectively. The ^1H NMR spectra are temperature invariant to −80 °C.

Attempted Preparation of $W_2(O\text{-}t\text{-}Bu)_6(C_3H_4)(py)_x$. $W_2(O\text{-}t\text{-}Bu)_6(C_3H_4)$ (250 mg, 295 mmol) was placed in a 30-mL Schlenk flask, which was then cooled to 0 °C. Pyridine was added with vigorous stirring until sufficient solvent had been added that all the solid just dissolved (~4 mL). The flask was then quickly warmed to room temperature to ensure complete dissolution of all solid and then cooled to −20 °C for 17 h. During this time green crystals formed, which were filtered at 0 °C to give 208 mg of product. The crystals were dried in vacuo, and a sample was examined by ^1H NMR spectroscopy for the presence of pyridine. Only the resonances expected for $W_2(O\text{-}t\text{-}Bu)_6(C_3H_4)$ were observed with no trace of pyridine. It was therefore concluded that $W_2(O\text{-}t\text{-}Bu)_6(C_3H_4)$ does not form a pyridine adduct.

$W_2(O\text{-}t\text{-}Bu)_6(MeC_3H_3)$. $W_2(O\text{-}t\text{-}Bu)_6$ (0.803 g, 0.996 mmol) was placed in a 50-mL Schlenk flask, and 3 mL of pentane was added. The contents of the flask were then frozen (−196 °C), evacuated, and transferred to the calibrated vacuum manifold. The solution was warmed to 0 °C and a large excess (~6 equiv) of methylallene was added. Slowly, the solution changed color on stirring at this temperature from red to deep green-brown. After stirring for 4 h at 0 °C, the flask was cooled to −78 °C for 15 h. During this time a green microcrystalline solid was formed and was filtered out at −78 °C, the filtrate being transferred to a flask cooled to 0 °C. The green solid obtained was dried in vacuo, and a portion was dissolved in toluene-d_8 at 0 °C for ^1H NMR spectroscopy.

^1H NMR data (300 MHz, 0 °C; toluene-d_8, δ): $C_3H_3(CH_3)$ 5.88 (d, $J_{H\text{-}H}$ = 2 Hz, 1 H), 5.79 (dq, $J_{H\text{-}HMe}$ = 6 Hz, $J_{H\text{-}H}$ = 2 Hz, 1 H), 5.10 (t, $J_{H\text{-}H}$ = 1.5 Hz, 1 H); $C_3H_3(CH_3)$ 2.74 (dt, $J_{H\text{-}H}$ = 6 Hz, $J_{H\text{-}H}$ = 2 Hz, 3 H); $OC(CH_3)_3$ 1.77 (s, 9 H), 1.72 (s, 9 H), 1.58 (s, 9 H), 1.50 (s, 9 H), 1.35 (s, 9 H), 1.32 (s, 9 H). The ^1H NMR spectrum was temperature invariant from 0 to −80 °C in toluene-d_8. However above 0 °C $W_2(O\text{-}t\text{-}Bu)_6(C_3H_3Me)$ reacts fairly slowly and after 5 h at room temperature the compound had completely rearranged to a large number of unidentified products.

$^{13}C\{^1H\}$ NMR data (74.5 MHz, 0 °C; toluene-d_8, δ): 222, 183.5, 120.4, 106.3, 87.5, 86.0, 84.2, 84.0, 83.7, 80.0, 38.2, 32.8, 31.8, 31.6, 30.7, 30.2.

IR data (cm^{-1}, Nujol mull): 1410 (w), 1370 (s), 1269 (w), 1235 (m), 1225 (m), 1200 (m), 1172 (s, br), 1090 (w), 1030 (m), 992 (m), 954 (s), 940 (s), 900 (s), 882 (s), 740 (w), 730 (w), 622 (w), 590 (w), 560 (m), 500 (w, sh), 500 (w), 482 (w), 400 (w, sh), 370 (w, br), 290 (w, br).

$[W(O\text{-}t\text{-}Bu)_3(C_3H_3Me)_2]_n$. The red-brown supernatant from the previous experiment which was separated from the green solid at −78 °C and transferred to a Schlenk flask at 0 °C was replaced at −20 °C for 18 h. During this time clusters of long orange needles grew. This solid was filtered, at 0 °C, into another Schlenk flask maintained at 0 °C. The Schlenk flask containing the supernatant was replaced at −20 °C and subsequently another crop of orange needles was obtained. The orange compound was dried in vacuo and then analyzed by NMR spectroscopic and combustion analytical techniques. These data are consistent with the empirical formula $[W(O\text{-}t\text{-}Bu)_3(C_3H_3Me)_2]$.

^1H NMR data (300 MHz, 23 °C; benzene-d_6, δ): C_3H_3Me 6.46 (dq, $J_{H(1)\text{-}H(5)}$ = 2.3 Hz, $J_{H(1)\text{-}H(5)}$ = 5.1 Hz, 1 H, H_1), 5.20 (q, $J_{H(2)\text{-}H(6)}$ = 6.4 Hz, 1 H, H_2), 3.87 (s, $J_{C\text{-}W}$ = 15 Hz, 2 H, H_3), 2.18 (dt, $J_{H(4)\text{-}H(5)}$ = 2.0 Hz, 3 H, H_4), 2.00 (br mult, 2 H, H_5), 1.87 (d, 3 H, H_6); $OC(CH_3)_3$ 1.67 (s, 9 H), 1.15 (s, 18 H). Coupling constants and multiplicities were determined from decoupling experiments and were confirmed by a 2D ^1H chemical shift correlated experiment.

^{13}C NMR data (125.8 MHz, 21 °C; benzene-d_6, δ): $C_3H_3CH_3$ 190.9 (s, $J_{C\text{-}W}$ = 44 Hz (14%), C_1), 150.0 (s, C_2), 119.2 (d, $J_{C\text{-}H}$ = 152 Hz, C_3), 116.5 (d, $J_{C\text{-}H}$ = 155 Hz, C_4), 45.7 (t, $J_{C\text{-}H}$ = 154 Hz, C_5), 36.8 (t, $J_{C\text{-}H}$ = 120 Hz, $J_{C\text{-}W}$ = 30 Hz (17%), C_6), 24.2 (q, $J_{C\text{-}H}$ = 125 Hz, C_7), 14.5 (q, $J_{C\text{-}H}$ = 124 Hz, C_8); $OCMe_3$ 83.9 (s), 76.7 (s); $OC(CH_3)_3$ 32.8 (q, $J_{C\text{-}H}$ = 125 Hz), 29.2 (q, $J_{C\text{-}H}$ = 126 Hz). Utilizing a 2D $^{13}C\text{-}^1H$ heteronuclear chemical shift correlated experiment optimized for $^1J_{C\text{-}H}$ established the following connectivities: C_3 is bonded to H_2; C_4 is bonded to H_1; C_5 is bonded to H_5; C_6 is bonded to H_3; C_7 is bonded to H_4; C_8 is bonded to H_6.

Anal. Calcd for $C_{20}H_{39}O_3W$; C, 46.96; H, 7.69. Found: C, 46.69; H, 6.94.

$W_2(O\text{-}t\text{-}Bu)_6(C_3H_4)_2$. $W_2(O\text{-}t\text{-}Bu)_6$ (0.510 g, 0.623 mmol) was placed in a 30-mL Schlenk flask equipped with a Teflon-coated stir bar, and 3 mL of hexane was added. The solution was stirred at room temperature for 15 min to break up the crystals of $W_2(O\text{-}t\text{-}Bu)_6$, after which time the flask was frozen at −196 °C and evacuated and allene (8.5 mmol) was added by using a calibrated vacuum manifold. The solution was warmed to 0 °C and stirred for 3 h, after which time the solution was cooled to −72 °C in a dry ice/ethanol bath overnight. The solution was removed by cannula transfer, and the green solid was dried in vacuo to give $W_2(O\text{-}t\text{-}Bu)_6(C_3H_4)_2$ (0.279 g, 0.315 mmol) in 50% yield. Crystals suitable for a single-crystal X-ray diffraction study were obtained from toluene at −72 °C.

^1H NMR (300 MHz, −10 °C; toluene-d_8, δ): C_3H_4 7.05 (dd, $^2J_{H\text{-}H}$ = 5 Hz, $^4J_{H\text{-}H}$ = 2 Hz, 1 H), 5.96 (dd, $^2J_{H\text{-}H}$ = 5 Hz, $^4J_{H\text{-}H}$ = 2 Hz, 1 H), 5.88 (d, $^4J_{H\text{-}H}$ = 3 Hz, 1 H), 5.15 (dd, $^2J_{H\text{-}H}$ = 5 Hz, $^4J_{H\text{-}H}$ = 3 Hz, 1 H), 3.96 (ddd, $^2J_{H\text{-}H}$ = 9 Hz, $^4J_{H\text{-}H}$ = 2 Hz, 2 Hz, 1 H), 3.64 (ddd, $^2J_{H\text{-}H}$ = 9 Hz, $^4J_{H\text{-}H}$ = 2 Hz, 2 Hz, 1 H), 2.77 (dd, $^2J_{H\text{-}H}$ = 5 Hz, $^4J_{H\text{-}H}$ = 3 Hz, 1 H), 2.40 (d, $^4J_{H\text{-}H}$ = 3 Hz, 1 H); $OC(CH_3)_3$ 1.76 (s, 9 H), 1.70 (s, 9 H), 1.56 (s, 9 H), 1.49 (s, 9 H), 1.40 (s, 9 H), 1.30 (s, 9 H).

$^{13}C\{^1H\}$ NMR (75.4 MHz, −10 °C; toluene-d_8, δ): $CH_2{=}C{=}CH_2$ 244.6, 195.7; $CH_2{=}C{=}CH_2$ 106.9; $OC(CH_3)_3$ 87.8; $CH_2{=}C{=}CH_2$ 86.8; $OC(CH_3)_3$ 84.8, 84.4, 84.1, 80.2, 77.8; $CH_2{=}C{=}CH_2$ 73.7; $OC(CH_3)_3$ 33.2, 32.2, 32.1, 31.0, 30.5; $CH_2{=}C{=}CH_2$ 29.0 ($J_{C\text{-}W}$ = 22 Hz (20%)).

IR (cm^{-1}, KBr): 2954 (vs), 2928 (s), 2918 (s), 2880 (sh), 2850 (sh), 1654 (w), 1462 (m), 1447 (m), 1379 (s), 1352 (vs), 1226 (s), 1188 (s), 1180 (s), 1120 (vs), 1090 (m), 1016 (m), 982–870 (vs), 848 (s), 778 (s), 770 (s), 718 (w), 574 (m), 543 (m), 518 (m), 484 (m), 470 (m), 460 (m), 360 (m).

$W_2(O\text{-}c\text{-}Hex)_6(C_3H_4)_2$. Yellow $W_2(O\text{-}c\text{-}Hex)_6$ (0.729 g, 0.75 mmol) was placed in a 50-mL Schlenk flask and suspended in 5 mL of toluene under a nitrogen atmosphere. The flask was then frozen at −196 °C and transferred to a calibrated vacuum manifold where it was evacuated and then allowed to warm to room temperature. An excess of allene was transferred into the flask until a pressure of 1 atm was maintained, with the flask open to a 75-mL vessel also containing 1 atm of allene. The solution slowly darkened to red-brown as it was stirred, and the yellow solid slowly dissolved. After about 2 h, a white rubbery precipitate had formed,

which was presumed to be polyallene. After stirring for a total of 8 h, the red-brown solution was filtered at room temperature and the solvent and excess allene removed in vacuo to give a dark brown oil. A ^{1}H NMR spectrum of the crude oil showed it to be essentially pure W_2(O-*c*-Hex)$_6$(C_3H_4)$_2$. By dissolving the oil in the minimum amount of 1,2-dimethoxyethane at room temperature (~6 mL) and cooling to −20 °C for 48 h, small green crystals were obtained. The crystals were filtered out and dried in vacuo, the volume of the filtrate was reduced by half, and the flask returned to the freezer at −20 °C. A second crop of crystalline material was obtained 3 days later. A total of 587 mg (0.56 mmol) of material was obtained, 74.7% isolated yield. The green material was determined to be W_2(O-*c*-Hex)$_6$(C_3H_4)$_2$ by NMR spectroscopy and combustion analysis.

^{1}H NMR data (300 MHz, 23 °C; benzene-d_6, δ): C_3H_4 2.82 (d, $J_{H(1)-H(3)}$ = 2.7 Hz, 1 H, H_1), 2.97 (dt, $J_{H(2)-H(4)}$ = 9.8 Hz, $J_{H(2)-H(7)}$ = 2.4 Hz, $J_{H(2)-H(8)}$ = 2.4 Hz, 1 H, H_2), 3.05 (dd, $J_{H(3)-H(5)}$ = 5.1 Hz, 1 H, H_3), 3.56 (dt, $J_{H(4)-H(7)}$ = 2.4 Hz, $J_{H(4)-H(8)}$ = 2.4 Hz, 1 H, H_4), 4.73 (dd, $J_{H(5)-H(6)}$ = 2.3 Hz, 1 H, H_5), 5.47 (d, J_{H-W} = 5.2 Hz, 1 H, H_6), 5.93 (m, $J_{H(7)-H(8)} \simeq$ 2.3 Hz, 1 H, H_7), 7.15 (m, 1 H, H_8) (coupling constants established by homonuclear decoupling experiments and chemical shifts correlated by a COSY experiment); OC*H* 5.15 (br mult, 3 H), 4.93 (m, 1 H), 4.84 (m, 1 H), 4.42 (m, 1 H); OCH(CH_2)$_5$ broad overlapping multiplets from 2.5 to 1.0. ^{1}H NMR (300 MHz, −30 °C; toluene-d_8, δ): C_3H_4 2.79 (H_1), 2.97 (H_2), 2.98 (H_3), 3.51 (H_4), 4.72 (H_5), 5.49 (H_6), 6.00 (H_7), 7.2 (H_8); OC*H* ~4.85 (v br), 4.92 (br), 4.80 (br), 4.38 (br). At −60 °C, all resonances of the compound were very broad but solvent resonances were still sharp and well resolved.

^{13}C NMR data (125.8 MHz, 21 °C; benzene-d_6, δ): 218.3 (s, J_{C-W} = 81 Hz (14%), C_1), 197.6 (s, J_{C-W} = 48 Hz (14%), C_2), 106.5 (t, J_{C-H} = 158 Hz, C_3), 85.5 (t, J_{C-H} = 155 Hz, C_4), 70.4 (t, J_{C-H} = 153 Hz, J_{C-W} = 28 Hz (14%), C_5), 29.5 (t, J_{C-H} = 153 Hz, J_{C-W} = 22 Hz (14%), C_6); OC*H* 84.7 (d), 82.5 (d), 78.4 (d), ~85 (v br), remaining resonances of cyclohexyl groups, overlapping singlets from δ 35 to 40 and 24 to 28. The following relationships were established by a 2D ^{13}C–^{1}H heteronuclear chemical shift correlated experiment, optimized to correlate one bond C–H interaction: C_3 is bonded to H_8 and H_7; C_4 is bonded to H_1 and H_3; C_5 is bonded to H_6 and H_5; C_6 is bonded to H_2 and H_4.

IR data (cm^{-1}, Nujol mull): 1370 (s), 1350 (m), 1320 (w), 1270 (w), 1155 (w), 1138 (w), 1098 (m), 1665 (s), 1055 (m, sh), 1040 (m), 1030 (m), 977 (s, br), 925 (w), 900 (w), 872 (w), 860 (w, sh), 852 (m), 805 (w), 730 (w), 700 (m), 692 (w), 565 (w), 540 (w), 470 (w).

Anal. Calcd for $C_{42}H_{74}O_6W_2$: C, 48.38; H, 7.15. Found: C, 48.21; H, 7.01.

W_2(O-*c*-Hex-d_{11})$_6$(C_3H_4)$_2$. This complex was prepared in a manner analogous to the above procedure from the reaction of W_2(O-*c*-Hex-d_{11})$_6$ with an excess of allene. The complex was isolated in a way similar to that described above except that a green-brown microcrystalline material was isolated from crystallization using 1,2-DME as solvent. The ^{1}H NMR spectroscopic data for the allene-derived protons were similar to those of the fully protio complex. No other allene-derived resonances were observed in the region that was previously obscured by the cyclohexyl protons.

Spin saturation transfer studies were run on W_2(O-*c*-Hex-d_{11})$_6$(C_3H_4)$_2$ in toluene-d_8 from room temperature to 50 °C, and no exchange was observed between allene protons.

IR data (cm^{-1}, Nujol mull): 2222 (s), 2120 (m), 1370 (m), 1265 (m), 1230 (m), 1212 (m), 1172 (s), 1135 (s), 1090 (s), 1077 (s), 1050 (s), 1028 (s), 980 (s, br), 935 (m), 920 (m), 882 (m), 872 (m), 800 (m, br), 745 (w), 728 (m), 722 (m), 695 (w), 672 (m), 645 (m), 630 (m, br).

Anal. Calcd for $C_{42}H_8D_{66}O_6W_2$: C, 45.51; H + D (as H), 6.68. Found: C, 45.37; H + D (as H), 6.95.

Reaction of W_2(O-*c*-Hex)$_6$(C_3H_4)$_2$ with Allene. W_2(O-*c*-Hex)$_6$(C_3H_4)$_2$ (35 mg, 0.035 mmol) was placed in a 25-mL Schlenk flask equipped with a Teflon-coated stir bar, and 10 mL of toluene was added. The flask was frozen at −196 °C, evacuated, and warmed to room temperature. The flask was stirred under an atmosphere of allene for 2 1/2 h with several additions of allene to maintain the pressure so that over 500 equiv were added. After this time, the allene pressure had stabilized and the flask was closed and allowed to stir overnight. The solvent and excess allene were removed in vacuo, and there was no evidence for the formation of polyallene. The ^{1}H NMR spectrum showed excusively unreacted W_2(O-*c*-Hex)$_6$(C_3H_4)$_2$.

W_2(O-*c*-Pen)$_6$(C_3H_4)$_2$. W_2(O-*c*-Pen)$_6$ (0.405 g, 0.40 mmol) was suspended in 4 mL of toluene at 0 °C in a 100-mL Schlenk flask. The flask was then frozen at −196 °C and evacuated, and then transferred to a calibrated vacuum manifold. The flask was warmed to 0 °C, and then allene was admitted until the pressure reached 1 atm. The yellow suspension turned deep red-brown on contact with the allene, and the yellow solid slowly dissolved over the course of about 1 h. The solution was stirred for a total of 5 h at 0 °C. During this time, a white insoluble precipitate formed, which was presumed to be polyallene. The solution was then filtered at room temperature, and the volatile components were removed from the filtrate in vacuo. A ^{1}H NMR spectrum of the crude red-brown oil indicated that the desired compound W_2(O-*c*-Pen)$_6$(C_3H_4)$_2$ had been formed in quantitative yield. The oil was taken up in a minimum amount of toluene (~1 mL) and cooled to −78 °C for 17 h. Since no solid was formed during this time, the solvent was removed at room temperature in vacuo and the oil was redissolved in 1 mL of pentane. After this solution was cooled for 20 h, a dark brown precipitate had formed, which was filtered out at −78 °C and dried in vacuo. W_2(O-*c*-Pen)$_6$(C_3H_4)$_2$ (264 mg, 0.28 mmol) was isolated in this way, a 70% yield.

^{1}H NMR data (300 MHz, 23 °C; toluene-d_8, δ): C_3H_4 2.53 (d, $J_{H(1)-H(2)}$ = 2.0 Hz, 1 H, H_1), 2.63 (dd, $J_{H(2)-H(5)}$ = 4.4 Hz, 1 H, H_2), 2.86 (dt, $J_{H(3)-H(4)}$ = 10.5 Hz, $J_{H(3)-H(7)}$ = 1.9 Hz, $J_{H(3)-H(8)}$ = 2.0 Hz, 1 H, H_3), 3.32 (dt, $J_{H(5)-H(7)}$ = 2.2 Hz, $J_{H(3)-H(8)}$ = 2.3 Hz, 1 H, H_4), 4.51 (dd, $J_{H(5)-H(6)}$ = 3.1 Hz, 1 H, H_5), 5.30 (d, 1 H, H_6), 5.79 (m, $J_{H(7)-H(8)}$ ~ 2.4 Hz, 1 H, H_7), 6.97 (m, 1 H, H_8); OC*H* 5.49 (m), 4.73 (m), ~5.4 (v br); OCH(CH_2)$_4$ broad overlapping multiplets from 2.0 to 1.2.

^{13}C{^{1}H} NMR data (75.4 MHz, 23 °C; toluene-d_8, δ): 220.4 (C_1), 197.7 (C_2), 106.2 (C_3), 88.4 (C_4), 70.0 (C_5), 31.7 (C_6); O*C*H 86.3, 88.3, 82.3, 81.2, ~87 (v br); OCH(CH_2)$_4$ overlapping singlets from 38 to 29.

Anal. Calcd for $C_{36}H_{62}O_6W_2$: C, 45.09; H, 6.52. Found: C, 45.01; H, 6.47.

W_2(O-*i*-Pr)$_6$(C_3H_4)$_2$. a. W_2(O-*i*-Pr)$_6$ was generated in situ by the following procedure. W_2(O-*t*-Bu)$_6$ (1.000 g, 1.24 mmol) was placed in a 50-mL Schlenk flask together with 3 mL of pentane. The solution was cooled to −78 °C in a dry ice/acetone bath and then an excess of dry 2-propanol (1.5 mL) was added dropwise over about 5 min. The solution was stirred for 2 h at −78 °C, after which time all the red color of W_2(O-*t*-Bu)$_6$ had disappeared and a pale yellow precipitate was present. The solution was filtered at −78 °C and washed with three 2-mL portions of hexane that had been precooled to −78 °C. The yellow solid that remained was dried in vacuo, first by pumping at −78 °C and then as it was warmed to room temperature to ensure that the final traces of HO-*i*-Pr had been removed. The pale yellow W_2(O-*i*-Pr)$_6$ so obtained was suspended in 2 mL of hexane at −78 °C (dry ice/acetone bath) and then cooled to −196 °C (liquid nitrogen). When the solution had frozen, the flask was evacuated and transferred to a calibrated vacuum manifold. The flask was warmed to −78 °C, and allene was admitted to the flask until the pressure of 1 atm was attained. The flask was then warmed to 0 °C in the presence of allene, and the pressure was adjusted until a pressure of 1 atm was again obtained. At 0 °C the yellow suspension of W_2(O-*i*-Pr)$_6$ rapidly reacted with allene to form a deep red solution. The mixture was stirred for 4 h at 0 °C, the solution was filtered to remove polymer, and then the volatile components were removed in vacuo to give a deep red oil. A ^{1}H NMR spectrum of the crude product indicated that the desired product had been formed and no other species were present. Repeated attempts to crystallize this compound from pentane, hexane, toluene, pyridine, or 1,2-dimethyloxyethane at low temperatures were unfruitful.

^{1}H NMR data (360 MHz, 26 °C; benzene-d_6, δ): C_3H_4 2.69 (d, $J_{H(1)-H(3)}$ = 2.3 Hz, 1 H, H_1), 2.82 (dt, $J_{H(2)-H(4)}$ = 9.8 Hz, $J_{H(2)-H(7)}$ = 2.6 Hz, $J_{H(2)-H(8)}$ = 2.7 Hz, 1 H, H_2), 2.87 (dd, $J_{H(3)-H(5)}$ = 4.8 Hz, 1 H, H_3), 3.42 (dt, $J_{H(4)-H(7)}$ = 2.6 Hz, $J_{H(4)-H(8)}$ = 2.7 Hz, 1 H, H_4), 2.62 (dd, $J_{H(5)-H(6)}$ = 2.4 Hz, 1 H, H_5), 5.42 (d, 1 H, H_6), 5.81 (m, $J_{H(7)-H(8)}$ = 2.3 Hz, 1 H, H_7), 7.16 (m, 1 H, H_8); OC*H*Me$_2$ 5.35 (br, 3 H), 5.28 (septet, 1 H), 5.17 (septet, 1 H), 4.72, (septet, 1 H); OCH(CH_3)$_2$ overlapping doublets from 1.2 to 1.8. The ^{1}H NMR spectrum of the two isolated four-proton spin systems of

the allene-derived resonances was successfully simulated by using the homonuclear coupling constants derived above from decoupling experiments and the observed chemical shifts in the Nicolet NMCSIM program.

^{13}C NMR data (75.4 and 125.8 MHz, 23 °C; toluene-d_8, δ): 218.2 (s, J_{C-W} = 80 Hz (14%), C_1), 197.1 (s, J_{C-W} = 48 Hz (14%), C_2), 106.3 (t, J_{C-H} = 158 Hz, C_3), 85.0 (t, C_4), 70.0 (t, J_{C-W} = 29 Hz (14%), C_5), 28.8 (t, J_{C-W} = 21 Hz (14%), C_6), OCH 78.6 (d), 73.7 (d), 71.5 (d), 78.5 (br); $OCH(CH_3)_2$ overlapping singlets from 22 to 28. The following connectivities were established by a 2D heteronuclear $^{13}C-^1H$ chemical shift correlated experiment optimized for $^1J_{C-H}$: C_3 is bonded to H_7 and H_8; C_4 is bonded to H_1 and H_3; C_5 is bonded to H_5 and H_6; C_6 is bonded to H_2 and H_4. A homonuclear chemical shift correlated experiment indicates that all the isopropoxide methyl groups are diastereotopic.

b. W_4(O-*i*-Pr)$_{12}$ (100 mg, 0.07 mmol) was reacted with an excess (1 atm) of allene in a 30-mL Schlenk flask with toluene as solvent. After stirring for 36 h at room temperature, the volatile components were removed in vacuo and the whole contents of the flask taken up in 0.5 mL of toluene-d_8. ^1H and ^{13}C NMR spectroscopy indicated that the same product as described under part a had been quantitatively formed.

c. W_2(O-*i*-Pr)$_6$(py)$_2$ (0.500 g, 0.6 mmol) was dissolved in 6 mL of hexane in a 50-mL Schlenk flask at room temperature. The flask was then frozen to −196 °C, evacuated, and transferred to a calibrated vacuum manifold. The flask was warmed to room temperature, and 1 atm of allene (a large excess) was transferred into the flask. The red-brown solution immediately changed color on contact with allene to give a solution that appeared deep green by reflected light, but deep red by transmitted light. After stirring for 2 h, the volatile components were removed in vacuo to give a dark red brown oil, which was pumped for a further 2 h under dynamic vacuum. A ^1H NMR spectrum of the crude oil showed only the presence of the same material prepared in part a above and no evidence for any pyridine resonances.

Precursors to $W_2(OR)_6(C_3H_4)_2$. $W_2(OR)_6(C_3H_4)_2$ (A). The ^1H NMR spectra of the reactions between $W_2(OR)_6$, R = O-*i*-Pr and O-*c*-Hex, and allene at room temperature after short reaction times provided evidence for an intermediate species in the formation of $W_2(OR)_6(C_3H_4)_2$. The intermediate species is spectroscopically similar to $W_2(OR)_6(C_3H_4)_2$ (R = O-*i*-Pr, O-*c*-Hex) and is believed to have the same empirical formula. This intermediate species is represented as $W_2(OR)_6(C_3H_4)_2$ (A).

W_2(O-*i*-Pr)$_6(C_3H_4)_2$ (A). ^1H NMR data (360 MHz, 26 °C; benzene-d_6, δ): C_3H_4 1.90 (dt, $J_{H(1)-H(4)}$ = 10 Hz, $J_{H(1)-H(7)}$ = 2.5 Hz, $J_{H(1)-H(8)}$ = 2.3 Hz, 1 H, H_1), 2.24 (s, 1 H, H_2), 3.01 (d, J_{H-H} = 4 Hz, 1 H, H_3), 3.42 (dt, $J_{H(4)-H(8)}$ = 2.3 Hz, $J_{H(4)-H(8)}$ = 2.4 Hz, 1 H, H_4), 5.10 (m, 1 H, H_5), 5.52 (d, J_{H-H} = 2.1 Hz, 1 H, H_6), 5.81 (m, $J_{H(7)-H(8)}$ = 2.5 Hz, 1 H, H_7), 7.07 (m, 1 H, H_8).

W_2(O-*c*-Hex)$_6(C_3H_4)_2$ (A). ^1H NMR data (360 MHz, 26 °C; benzene-d_6, δ): C_3H_4 2.35 (d, 1 H, H_1), 2.60 (dt, 1 H, H_2), 3.15 (d, 1 H, H_3), 3.58 (dt, 1 H, H_4), 5.20 (dd, 1 H, H_5), 5.52 (d, 1 H, H_6), 5.83 (d, 1 H; H_7), 7.06 (s, 1 H, H_8).

On standing in solution at room temperature the complexes $W_2(OR)_6(C_3H_4)_2$ (A) (R = O-*i*-Pr and O-*c*-Hex) quantitatively rearrange to their isolable counterparts, $W_2(OR)_6(C_3H_4)_2$ (same R) as described above. Attempts to isolate the intermediate species on a preparative scale by conducting reactions between $W_2(OR)_6$ and allene at 0 °C for short reaction periods (i.e. 20 min) resulted only in formation of mixtures of $W_2(OR)_6(C_3H_4)_2$ (A) and $W_2(OR)_6(C_3H_4)_2$.

^1H NMR Studies of W_2(O-*c*-Hex-d_{11})$_6$ (A). The Kinetic Product. W_2(O-*c*-Hex-d_{11})$_6$ (10 mg, 0.01 mmol) was dissolved in 0.5 mL of toluene-d_8, 0.02 mmol of allene was added with a calibrated vacuum manifold, and the NMR tube was sealed. The solution was allowed to warm to room temperature for 5 min, and the solution NMR studies were carried out within 2 h at −20 or 0 °C, after which time the sample had substantially rearranged to form the thermodynamic product.

^1H NMR (0 °C; toluene-d_8, δ): 2.01 (m, 1 H, H_1), 2.34 (s, 1 H, H_2), 3.13 (d, 1 H, H_3), 3.51 (m, 1 H, H_4), 5.19 (dd, 1 H, H_5), 5.52 (d, 1 H, H_6), 5.85 (dd, 1 H, H_7), 7.76 (d, 1 H, H_8).

COSY studies show a coupling pattern similar to that of the thermodynamic product.

The briding allene is indicated by H_6 coupling to H_5, which couples to H_6 and H_3. The geminal pair for H_3 is H_2, which was a singlet, so no geminal coupling was observed. The terminally bound allene had a coupling pattern very similar to that of the thermodynamic product. H_8 and H_7 were multiplets and geminal pairs, coupling to each other and to H_4 and H_1, which showed an additional geminal coupling to each other.

Nuclear Overnhauser enhancement (NOE) studies were done at −20 °C in toluene-d_8 by using a delay time of 5 s. Forty scans were collected with four collected with decoupling at the point of interest and then four collected with decoupling at a point far off resonance until 40 scans were collected for each decoupling frequency. The spectra were then subtracted to give a difference spectrum. NOE (10–20%) was observed between all geminal protons and (3–5%) between the interior protons of the bridging allene groups, H_6 and H_2 for the kinetic product, and H_6 and H_1 for the thermodynamic product. Interallene NOE (5–6%) was observed between H_2 and H_4 in the kinetic product and between H_7 and H_8 in the thermodynamic product.

$W_2(OCH_2$-*t*-Bu$)_6 + C_3H_4$. $W_2(OCH_2$-*t*-Bu$)_6$ reacts with allene at room temperature to form initially a compound analogous to $W_2(OR)_6(C_3H_4)_2$ (A) described above, which then rearranges to form ^1H NMR resonances consistent with $W_2(OR)_6(C_3H_4)_2$ (R = O-*i*-Pr, O-*c*-Pen, O-*c*-Hex) as described above. However, on standing at room temperature, this compound rearranges to other unidentified species.

$W_2(OCH_2$-*t*-Bu$)_6(C_3H_4)_2$ (A). ^1H NMR data (300 MHz, 23 °C; toluene-d_8, δ): C_3H_4 obscured (H_1), 2.29 (s, 1 H, H_2), 3.08 (d, J_{H-H} = 3.9 Hz, 1 H, H_3), 3.46 (dt, J_{H-H} = 10.5 Hz, 1 H, H_4), 5.15 (dd, J_{H-H} = 1.8 Hz, 1 H, H_5), 5.78 (m, 1 H, H_7), 6.98 (m, 1 H, H_8).

$W_2(OCH_2$-*t*-Bu$)_6(C_3H_4)_2$. ^1H NMR data (300 MHz, 23 °C; toluene-d_8, δ): 2.70 (d, 1 H, H_1), 2.98 (dt, 1 H, H_2), 2.95 (dd, 1 H, H_3), 3.46 (dt, 1 H, H_4), 4.69 (dd, 1 H, H_5), 5.36 (dd, 1 H, H_6), 5.83 (m, 1 H, H_7), 7.03 (m, 1 H, H_8).

Preparation of W_2(O-*c*-Pen$)_6(C_3H_4)_2(HNMe_2)$. W_2(O-*c*-Pen$)_6(C_3H_4)_2$[22] (200 mg, 0.206 mmol) was placed in a 30-mL Schlenk flask equipped with a Teflon-coated stir bar, and 10 mL of hexanes was added. The solution was frozen at −196 °C, the flask was evacuated, and 3 mmol of allene was added via a calibrated vacuum manifold. The solution was allowed to warm to room temperature, back-filled with N_2(g) and stirred overnight. The solution was cooled to −20 °C for 48 h, and black crystals of W_2(O-*c*-Pen$)_6(C_3H_4)_2(HNMe_2)$ (69 mg, 0.069 mmol) were isolated in 33% yield. The solid was thermally unstable at room temperature, presumably by dissociation of $HNMe_2$ to form W_2(O-*c*-Pen$)_6(C_3H_4)_2$.

^1H NMR (500 MHz, 25 °C; toluene-d_8, δ): C_3H_4 2.60 (d, J_{H-H} = 2 Hz, 1 H), 2.67 (dd, $^2J_{H-H}$ = 5 Hz, $^4J_{H-H}$ = 2 Hz, 1 H), 2.90 (dt, $^2J_{H-H}$ = 10 Hz, $^4J_{H-H}$ = 3 Hz, 1 H), 3.37 (dt, $^2J_{H-H}$ = 10 Hz, $^4J_{H-H}$ = 3 Hz, 1 H), 4.56 (dd, $^2J_{H-H}$ = 5 Hz, $^4J_{H-H}$ = 2 Hz, 1 H), 5.36 (d, J_{H-H} = 2 Hz, 1 H), 5.85 (dd, J_{H-H} = 2 Hz, J_{H-H} = 2 Hz, 1 H), 7.05 (d, J_{H-H} = 2 Hz, 1 H); *H*NMe_2 4.79 (m, 1 H); HN*Me*$_2$ 2.42 (m, 3 H), 2.54 (m, 3 H); O-*c*-C_5H_9, α-H 5.53 (m, 3 H), 4.75 (m, 3 H); O-*c*-C_5H_9, CH_2 2.03–1.22 (overlapping mult, 48 H). At 60 °C, the ^1H NMR resonances for C_3H_4 are identical with those found for W_2(O-*c*-Pen$)_6(C_3H_4)_2$.

IR data (cm^{-1}, KBr): 2920 (s), 2836 (m), 2326 (w), 2320 (w), 1442 (w), 1430 (w), 1354 (w), 1328 (m), 1160 (m), 1062 (m), 1030 (m), 988 (s), 929 (w), 913 (w), 861 (m), 676 (w), 600 (w), 546 (w).

Anal. Calcd for $C_{38}H_{69}NO_6W_2$: C, 45.47; H, 6.93; N, 1.40. Found: C, 44.88; H, 6.47; N, 0.63. Calcd for $C_{36}H_{62}O_6W_2$(W_2(O-*c*-Pen$)_6(C_3H_4)_2$): C, 45.09; H, 6.52.

W_2(O-*t*-Bu$)_6(C_3H_4)(CO)_2$. W_2(O-*t*-Bu$)_6(C_3H_4)$ was synthesized as above starting with W_2(O-*t*-Bu$)_6$ (0.510 g, 0.632 mmol). After stirring for 2 h under an allene atmosphere, the solvent was removed in vacuo at 0 °C and then 2 mL of hexane was added at −78 °C. The solution was frozen at −196 °C, evacuated, warmed to 0 °C, then opened to 1 of CO, and stirred for 1 h. The flask was back-filled with nitrogen and cooled to −15 °C overnight. W_2(O-*t*-Bu$)_6(C_3H_4)(CO)_2$ (237 mg, 0.263 mmol) was isolated as red crystals in 42% yield. Crystals suitable for a single-crystal X-ray diffraction study were obtained from hexane at −20 °C.

^1H NMR (360 MHz, 22 °C; toluene-d_8, δ): $OC(CH_3)_3$ 1.35 (s, 9 H), 1.47 (s, 18 H), 1.61 (s, 18 H), 1.78 (s, 9 H); C_3H_4 3.60 (s, 2 H), 4.05 (s, 2 H).

(22) Chacon, S. T.; Chisholm, M. H.; Folting, K.; Hampden-Smith, M. J.; Huffman, J. C. *Inorg. Chem.* **1991**, *30*, 3122.

Table IX. Summary of Crystal Data

	1	2	3
empirical formula	$C_{27}H_{58}O_6W_2$	$W_2O_6C_{30}H_{62}$	$W_2C_{29}H_{58}O_8$
cryst color	dark green	dark green	dark red
cryst dimens, mm	0.25 × 0.22 × 0.29	0.068 × 0.18 × 0.242	0.25 × 0.25 × 0.25
space group	$P2_1/n$	$P2_1/c$	$P2_1/c$
cell dimens			
temp, °C	−144	−155	−155
a, Å	11.676 (1)	9.516 (3)	15.823 (4)
b, Å	16.771 (2)	19.114 (7)	18.807 (5)
c, Å	17.116 (2)	19.438 (6)	22.457 (6)
β, deg	90.39 (0)	103.32 (2)	90.93 (1)
Z (molecules/cell)	4	4	8
V, Å^3	3351.33	3440.41	6681.93
calcd dens, gm/cm^3	1.678	1.715	1.749
λ, Å	0.710 69	0.710 69	0.710 69
mol wt	846.45	886.52	902.47
linear abpt coeff, cm^{-1}	70.392	68.760	71.099
detector to sample dist, cm	22.5	22.5	22.5
sample to source dist, cm	23.5	23.5	23.5
av ω scan width at half-height	0.25	0.25	0.25
scan speed, deg/min	6.0	6.0	6.0
scan width, deg + dispersion	1.8	2.0	1.8
individual background, s	6	6	6
aperture size, mm	3.0 × 4.0	3.0 × 4.0	3.0 × 4.0
2θ range, deg	6–45	6–45	6–45
total no. of reflns collcd	8830	5957	9384
no. of unique intensities	4397	4503	8714
no. of with $F > 0.0$	4203	4179	7336
no. of with $F > 2.33\sigma(F)$		3867	3500
no. of with $F > 3.0\sigma(F)$	4035		
$R(F)$	0.0309	0.0383	0.0714
$R_w(F)$	0.0293	0.0368	0.0728
goodness of fit for last cycle	1.373	1.129	1.642
max. δ/σ for last cycle	0.05	0.35	0.45

^{13}C NMR (75.4 MHz, 22 °C; benzene-d_6, δ): $OC(CH_3)_3$ 31.3 (q, $^1J_{CH}$ = 130 Hz, 3 C), 31.7 (q, $^1J_{CH}$ = 120 Hz, 3 C), 33.1 (q, $^1J_{CH}$ = 130 Hz, 6 C), 34.9 (q, $^1J_{CH}$ = 120 Hz, 3 C); CH_2CCH_2 67.9 (dddd, $^1J_{CH}$ = 160 Hz, $^1J_{CH'}$ = 150 Hz, $^3J_{CH}$ = 5 Hz, $^3J_{CH}$ = 5 Hz, 2 C); $OC(CH_3)_3$ 78.7 (s, 1 C), 80.1 (s, 1 C), 82.3 (s, 2 C), 88.8 (s, 2 C); CH_2CCH_2 177.1 (s, 1 C); CO 212.0 (s, 2 C).

IR (cm^{-1}, KBr): 2954 (s), 2920 (sh), 2904 (sh), 2850 (sh), 1900 (s) (CO), 1830 (s) (CO), 1464 (w), 1446 (m), 1355 (s), 1348 (sh), 1254 (m), 1228 (m), 1168 (s), 1154 (s), 1090 (w), 1015 (m), 1008 (sh), 974 (s), 925 (s, br), 880 (s), 860 (s), 775 (s), 718 (sh), 550 (m), 480 (w), 470 (sh), 376 (w). $R_{sym}(CO)/R_{asym}(CO)$ = 1.6.

Anal. Calcd for $C_{29}H_{58}O_8W_2$: C, 38.59; H, 6.49. Found: C, 38.11; H, 6.24.

W_2(O-*t*-Bu)$_6$(C_3H_4)(^{13}CO)$_2$. This was made as above, starting with W_2(O-*t*-Bu)$_6$ (2.112 g, 2.619 mmol) and adding allene and then 4 equiv of ^{13}CO. The solvent was removed in vacuo, the red solid was recrystallized from toluene at −15 °C, and 632 mg (0.699 mmol) was isolated in 27% yield.

^{1}H NMR (300 MHz, 22 °C; benzene-d_6, δ): C_3H_4 4.08 (s, 2 H), 3.67 (t, $^3J_{HC}$ = 5 Hz, 2 H).

^{13}C{^{1}H} NMR (75.4 MHz, 22 °C; benzene-d_6, δ): CO 212.0 ($^1J_{CW}$ = 180 Hz (14%), 2 C).

IR (cm^{-1}, KBr): 1855 (s) (CO), 1778 (m) (CO).

W_2(O-*c*-Hex)$_6$(C_3H_4)$_2$ + CO. W_2(O-*c*-Hex)$_6$(C_3H_4)$_2$ (340 mg, 0.326 mmol) was placed in a 25-mL Schlenk flask equipped with a Teflon-coated stir bar, and 15 mL of hexane was added by cannula transfer. CO (0.326 mmol) was added by gastight syringe, and the solution was stirred for 3 h at room temperature. The solution was then cooled to −20 °C overnight and 50 mg, 0.047 mmol, of brown crystals were isolated in 14% yield. The similarity of the ^{1}H NMR spectrum to 3 led us to formulate this as W_2(O-*c*-Hex)$_6$(C_3H_4)(CO)$_2$.

^{1}H NMR (75.4 MHz, 22 °C; benzene-d_6, δ): O-*c*-Hex, α-H 5.0–4.7 (br, 6 H); C_3H_4 4.03 (s, 2 H), 3.78 (s, 2 H); O-*c*-Hex, CH_2 1.69–0.76 (overlapping mult, 60 H).

W_2(O-*c*-Hex)$_6$(C_3H_4)$_2$ + 6^{13}CO. W_2(O-*c*-Hex)$_6$(C_3H_4)$_2$ (16 mg, 0.015 mmol) was placed in an NMR tube, 0.5 mL of benzene was added, and then 0.092 mmol of ^{13}CO was added by gastight syringe. The solution was left for 1 h before spectra were run. The ^{13}C resonance at δ 210.9 was assigned to W_2(O-*c*-Hex)$_6$(C_3H_4)(CO)$_2$ due to its similarity to 3, and the ^{13}C resonance at δ 263.7 was assigned to W_2(O-*c*-Hex)$_6$(C_3H_4)$_2$(CO) due in part to the appearance of eight inequivalent allene proton resonances in the ^{1}H NMR spectrum.

^{13}C{^{1}H} NMR (75.4 MHz, 22 °C; benzene-d_6, δ): 210.9 ($J_{^{13}C-^{183}W}$ = 180 Hz (17%)), 263.7 ($J_{^{13}C-^{183}W}$ = 190 Hz (22%)).

^{1}H NMR (300 MHz, 22 °C; benzene-d_6, δ): 5.09–4.92 (m, 4 H), 4.76 (m, 1 H), 4.56 (m, 1 H), 4.50 (s, 1 H), 4.46 (m, 1 H), 4.44 (m, 2 H), 4.39 (m, 1 H), 4.16 (m, 1 H), 4.03 (s, 2 H), 3.98 (m, 1 H), 3.95 (m, 1 H), 3.78 (s, 2 H).

W_2(O-*c*-Hex-d_{11})$_6$(C_3H_4)$_2$ + 6CO. W_2(O-*c*-Hex-d_{11})$_6$(C_3H_4)$_2$ (12 mg, 0.011 mmol) was placed in an NMR tube, 0.5 mL of benzene was added, and 0.065 mmol of CO was added by gas-tight syringe. The NMR spectrum was run after 1 h at room temperature.

^{1}H NMR (300 MHz, 22 °C; benzene-d_6, δ): W_2(O-*c*-Hex)$_6$(C_3H_4)$_2$(CO)$_2$ 5.03 (m, 1 H), 4.76 (m, 1 H), 4.56 (m, 1 H), 4.50 (s, 1 H), 4.46 (m, 1 H), 4.44 (m, 1 H), 3.98 (m, 1 H), 3.95 (m, 1 H); W_2(O-*c*-Hex)$_6$(C_3H_4)(CO)$_2$ 4.03 (s, 2 H), 3.78 (s, 2 H).

Crystallographic Studies

General operating procedures and listings of programs have been described previously.[23] A summary of crystal data is given in Table IX.

W_2(O-*t*-Bu)$_6$(C_3H_4) (1). A small, almost equidimensional, crystal was selected from the air- and moisture-sensitive sample. The crystal was transferred to the goniostat, where it was cooled to −144 °C for characterization and data collection. A systematic, computerized search of a limited hemisphere of reciprocal space ($4 < 2\theta < 8$) yielded a set of 23 centered reflections that exhibited monoclinic symmetry. The systematic extinction of $0k0$ for $k = 2n + 1$ and of $h0l$ for $h + l = 2n + 1$ identified the space group as $P2_1/n$. This choice was confirmed by the successful solution and refinement of the structure.

The structure was solved by using a combination of direct methods and Fourier techniques. The two W atoms were readily located and the remainder of the non-hydrogen atoms appeared

(23) Chisholm, M. H.; Folting, K.; Huffman, J. C.; Kirkpatrick, C. C. *Inorg. Chem.* **1984**, *23*, 1021.

in a difference Fourier map phased with the W atoms. Almost all of the hydrogen atoms on the methyl groups were located in a later difference map. The four hydrogen atoms on the allene ligand were located in a subsequent difference map. The full-matrix least-squares refinement was completed by using anisotropic thermal parameters on all non-hydrogen atoms and isotropic thermal parameters on the hydrogen atoms.

The final difference Fourier map was essentially featureless except for two peaks of 1.5 and 1.2 e/Å^3 in the immediate vicinity of the two tungsten atoms.

W_2(O-*t*-Bu)$_6$(C_3H_4)$_2$ (2). A suitable crystal was located, transferred to the goniostat, and cooled to −155 °C for characterization and data collection.

A systematic search of a limited hemisphere of reciprocal space located a set of diffraction maxima with symmetry and systematic absences corresponding to the unique monoclinic space group $P2_1/c$. Subsequent solution and refinement of the structure confirmed this choice.

Data were collected in the usual manner using a continuous θ–2θ scan with fixed backgrounds. Data were reduced to a unique set of intensities and associated σ's in the usual manner. Data were corrected for absorption. The structure was solved by a combination of direct methods (MULTAN78) and Fourier techniques. All hydrogen atoms were clearly visible in a difference Fourier synthesis phased on the non-hydrogen parameters. All hydrogen atoms were refined isotropically and non-hydrogen atoms anisotropically in the final cycles.

A final difference Fourier was featureless, with several peaks of intensity 0.8–1.1 e/Å^3 lying near the metal atoms.

W_2(O-*t*-Bu)$_6$(C_3H_4)(CO)$_2$ (3). The crystalline sample consisted of "clumps" of black crystals with poorly defined faces. Several attempts were made before a suitable fragment was located. Many of the crystals examined were badly split (or twinned), as evidenced by numerous closely grouped peaks. The sample was maintained in a dry nitrogen atmosphere by using standard techniques employed by the Indiana University Molecular Structure Center.

A systematic search of a limited hemisphere of reciprocal spaces located a set of diffraction maxima with symmetry and systematic absences corresponding to the unique monoclinic space group $P2_1/c$. It was apparent that a significant "pseudocell" was present, as seen in the intensity distribution. The $h0l$ zone, for example, is best described as present for $l = 4n$. Unfortunately, the exceptions to the "extinctions" were clearly present, so it was not possible to simply reduce the cell.

Data were collected by using a continuous θ–2θ scan with fixed backgrounds. Data were reduced to a unique set of intensities and associated σ's in the usual manner. The structure was solved by a combination of direct methods (MULTAN78) and Fourier techniques. As expected, two independent molecules are present in the unique quadrant. Because of the pseudocell, less than half of the unique data were observed. For this reason, no attempt was made to refine anisotropically any atoms except the tungsten atoms.

The two molecules are nearly identical, as evidenced by their similar metric parameters.

Acknowledgment. We thank the Department of Energy, Office of Basic Sciences, Chemistry Division, for financial support.

Supplementary Material Available: For the compounds W_2(O-*t*-Bu)$_6$(C_3H_4), W_2(O-*t*-Bu)$_6$(C_3H_4)$_2$, and W_2(O-*t*-Bu)$_6$(C_3H_4)(CO)$_2$, complete listings of atomic coordinates, anisotropic thermal parameters, and bond distances and angles and stereoviews (50 pages); F_o and F_c values (38 pages). Ordering information is given on any current masthead page.

Dynamic Processes in the Solid State. Diene Flip and Ring Reorientation in Crystalline Zirconocene Complexes

Dario Braga,* Fabrizia Grepioni, and Emilio Parisini

Dipartimento di Chimica "G. Ciamician", Università di Bologna, Via Selmi 2, 40126 Bologna, Italy

Received March 13, 1991

The dynamic processes that the zirconocene species $(C_5H_5)_2ZrCl_2$ (1), $(C_5H_4{}^tBu)_2ZrCl_2$ (2), $(C_5H_5)_2ZrC_4H_4Me_2$ (3), and $(C_5H_4{}^tBu)_2ZrC_4H_6$ (4) undergo in the solid state have been examined. The results of potential energy barrier calculations and packing analyses are discussed in light of the dynamic information obtained by ^{13}C magic angle spinning NMR spectroscopy. The potential energy barriers to reorientation of the C_5H_5 ligands in 1 and 3 are estimated, while the $C_5H_4{}^tBu$ groups in 2 and 4 are found to be blocked in their motion. An alternative interpretation of the diene flip, detected in 3 and 4 by the NMR experiments, is put forward.

Introduction

In previous papers[1] we have shown that the pairwise atom–atom potential energy method[2] can be fruitfully used to investigate the occurrence of dynamic processes in crystals of neutral organometallic molecules. The method affords a clear picture of the control exerted by the crystal packing on the reorientational motions that metal-bound molecular fragments can undergo in the solid state. A (semi)quantitative estimate of the potential energy (pe) barriers opposing the reorientational motions can also be attained in most cases. The potential energy approach becomes particularly useful when complementary information on the dynamic processes can be obtained from spectroscopic sources. ^{13}C CP/MAS NMR and ^1H wide-line experiments or spin–lattice relaxation time measurements are well-suited for the investigation of solid-state reorientational phenomena.[3] Successful correlations be-

(1) (a) Braga, D.; Gradella, C.; Grepioni, F. *J. Chem. Soc., Dalton Trans.* **1989**, 1721. (b) Braga, D.; Grepioni, F. *Polyhedron* **1990**, *1*, 53. (c) Braga, D.; Grepioni, F.; Johnson, B. F. G.; Lewis, J.; Martinelli, M. *J. Chem. Soc., Dalton Trans.* **1990**, 1847. (d) Aime, S.; Braga, D.; Gobetto, R.; Grepioni, F.; Orlandi, A. *Inorg. Chem.* **1991**, *30*, 951. (e) Braga, D.; Grepioni, F. *J. Chem. Soc., Dalton Trans.* **1990**, 3143. (f) Braga, D.; Grepioni, F. *Inorg. Chem.*, submitted for publication. (g) Braga, D.; Bürgi, H.-B.; Grepioni, F.; Raselli, A. *Acta Crystallogr.*, submitted for publication.

(2) (a) Kitaigorodsky, A. I. *Molecular Crystals and Molecules*; Academic Press: New York, 1973. (b) Pertsin, A. J.; Kitaigorodsky, A. I. *The Atom-Atom Potential Method*; Springer-Verlag: Berlin, 1987.

0276-7333/91/2310-3735$02.50/0